



Published in final edited form as:

Eur J Med Chem. 2023 November 15; 260: 115772. doi:10.1016/j.ejmech.2023.115772.

Structure and Function of SARS-CoV and SARS-CoV-2 Main Proteases and Their Inhibition: A Comprehensive Review

Xin Li^{1,2,*}, Yongcheng Song^{1,2,*}

¹Department of Pharmacology and Chemical Biology, Baylor College of Medicine, 1 Baylor Plaza, Houston, TX 77030, USA.

²Dan L. Duncan Comprehensive Cancer Center, Baylor College of Medicine, 1 Baylor Plaza, Houston, TX 77030, USA.

Abstract

Severe acute respiratory syndrome-associated coronavirus (SARS-CoV) identified in 2003 infected ~8,000 people in 26 countries with 800 deaths, which was soon contained and eradicated by syndromic surveillance and enhanced quarantine. A closely related coronavirus SARS-CoV-2, the causative agent of COVID-19 identified in 2019, has been dramatically more contagious and catastrophic. It has infected and caused various flu-like symptoms of billions of people in >200 countries, including >6 million people died of or with the virus. Despite the availability of several vaccines and antiviral drugs against SARS-CoV-2, finding new therapeutics is needed because of viral evolution and a possible emerging coronavirus in the future. The main protease (M^{pro}) of these coronaviruses plays important roles in their life cycle and is essential for the viral replication. This article represents a comprehensive review of the function, structure and inhibition of SARS-CoV and -CoV-2 M^{pro}, including structure-activity relationships, protein-inhibitor interactions and clinical trial status.

Graphical Abstract

* **CORRESPONDING AUTHOR:** To whom correspondence should be addressed. Address: Department of Pharmacology and Chemical Biology, Baylor College of Medicine, 1 Baylor Plaza, Houston, TX 77030. xin.li2@bcm.edu (X. L.) or ysong@bcm.edu (Y. S.).

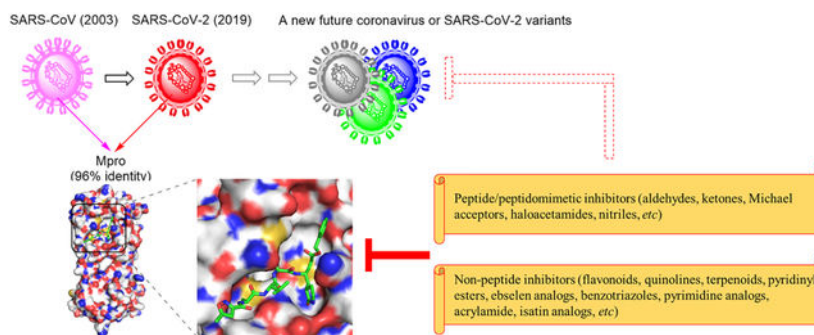
Publisher's Disclaimer: This is a PDF file of an unedited manuscript that has been accepted for publication. As a service to our customers we are providing this early version of the manuscript. The manuscript will undergo copyediting, typesetting, and review of the resulting proof before it is published in its final form. Please note that during the production process errors may be discovered which could affect the content, and all legal disclaimers that apply to the journal pertain.

Competing interests

The authors declare that they have no competing interests.

Declaration of interests

The authors declare that they have no known competing financial interests or personal relationships that could have appeared to influence the work reported in this paper.



Keywords

SARS-CoV-2; Main protease; Small-molecule inhibitor; Drug discovery

1. Introduction

Severe acute respiratory syndrome (SARS) is caused by SARS-associated coronavirus (SARS-CoV), a novel coronavirus identified in 2003. Its outbreak resulted in >8,000 cases including >800 deaths in 26 countries worldwide [1]. Without an effective treatment, SARS-CoV infection had a high mortality rate of ~10%. It was soon contained and eradicated through syndromic surveillance and enhanced quarantine. A closely related coronavirus SARS-CoV-2, the causative agent of COVID-19 discovered in Wuhan, China in December of 2019, has been dramatically more pandemic and catastrophic in the history of public health [2]. SARS-CoV-2 is highly contagious with an estimated basic reproductive number R_0 of 5.7, significantly higher than ~3 for SARS-CoV and ~1.5 for H1N1 influenza (swine flu) in 2009 [3]. It has rapidly spread to more than 200 countries worldwide and infected and caused various flu-like symptoms of billions of people worldwide, including >6 million people (mostly elderly) died of or with the virus. In addition to upper and lower respiratory system, SARS-CoV-2 affects multiple other organs, including heart, kidney, liver and gastrointestinal and central nervous system [4]. Facing such a devastating health crisis, most countries enforced various types of “Stay at Home” orders to restrict the spread of the virus, which caused enormous negative impact to the economy. Despite the availability of several effective vaccines and antiviral drugs against SARS-CoV-2 [5], studies towards finding new targeted therapeutics are needed because of continued evolution of SARS-CoV-2 and a possible emerging coronavirus in the future.

SARS-CoV-2 is highly homologous to SARS-CoV with 82% identity in their genome sequences, particularly for several essential enzymes such as RNA-dependent RNA polymerase (RdRp, with 96% identity) and main protease (M^{pro}, with 96% identity) [6]. Studies have shown various viral and host proteins play critical roles in different stages of the life cycle of SARS-CoV-2, including the viral spike protein, RdRp, M^{pro} and papain-like protease (PL^{pro}) as well as host angiotensin-converting enzyme 2 (ACE2), cyclophilins and several other proteins [7]. Among these, M^{pro} is a promising drug target for development of antiviral agents against SARS-CoV and -CoV-2, since M^{pro} can generate 11 non-structural viral proteins [8] and is essential for replication of these viruses. This article reviews the

function, structure and inhibitors of SARS-CoV and SARS-CoV-2 M^{pro}, including protein-inhibitor interactions, structure-activity relationships, and clinical trial status. In addition, the perspectives of the antiviral drug discovery and development targeting M^{pro} of SARS-CoV-2 and closely related coronaviruses are discussed.

2. SARS-CoV, SARS-CoV-2 and other Coronavirus family members

SARS-CoV and SARS-CoV-2 belong to the Coronavirus family of RNA viruses [9], which contain four genera: α -, β -, γ -, and δ -coronavirus. α - and β -Coronavirus only infect mammals, while γ - and δ -coronavirus primarily infect birds [10]. To date, seven coronaviruses causing human diseases have been identified, including HCoV-229E, HCoV-NL63, HCoV-OC43, HCoV-HKU1, SARS-CoV, MERS-CoV, and SARS-CoV-2 [11, 12]. Phylogenetic analysis suggests all of these human coronaviruses originate from animals. HCoV-229E and HCoV-NL63 belong to α -coronavirus, while HCoV-OC43 and HCoV-HKU1 are β -coronavirus. These 4 viruses cause about one-third of common colds in humans [13] with generally mild symptoms, but they may occasionally lead to severe pneumonia and bronchiolitis in infants [14] and immunocompromised patients [15–17] or be associated with certain enteric diseases [18] and neurological disorders [19–21]. Recently identified SARS-CoV, MERS-CoV and SARS-CoV-2 are β -coronaviruses and far more pathogenic, causing serious and sometimes fatal respiratory diseases in humans.

SARS-CoV and SARS-CoV-2 are positive-sense, single-stranded RNA viruses with a genome size of 29.7 and 29.9 kb, respectively [22, 23]. Their RNA and the associated nucleocapsid proteins form a capsid [24], which is enveloped by a bilayer lipid membrane studded with the viral envelope and spike proteins (Figure 1a). The SARS-CoV and SARS-CoV-2 genomes contain an untranslated region at both the 5'- and 3'-terminus and several open reading frames (ORF) (Figure 1b). The life cycle of SARS-CoV-2 (or SARS-CoV) begins with its attachment to the host cells [9, 23, 25–27], through the interactions between its spike protein and the host cell surface ACE2 [28]. The binding triggers fusion of the viral and host cell membranes followed by endocytosis and releasing the viral RNA into the host cytoplasm, where it is translated into viral proteins. ORF1a and its frameshifted ORF1a/b give two large polyproteins, pp1a (~450 kDa) and pp1ab (~750 kDa) [8, 29], which are site-specifically cleaved by the viral proteases PL^{pro} (i.e., nsp3) and M^{pro} (nsp5) to produce 16 viral non-structure proteins (nsp), including the two proteases and RdRp (nsp12). The other RNA sequences are translated to generate viral structural proteins including the spike, envelope, membrane, nucleocapsid protein and several accessory proteins. In the meantime, RdRp is used to replicate the viral genomic RNA, which is complexed with the nucleocapsid proteins to form a capsid in the host endoplasmic reticulum-Golgi intermediate compartment (ERGIC), where a new virus particle is assembled and ready for egress to infect a new cell.

3. Structure and function of SARS-CoV and -CoV-2 M^{pro}

SARS-CoV or -CoV-2 M^{pro} (also known as 3CL^{pro}), which cleaves the viral polyprotein and generates 11 non-structure viral proteins [8], is essential for replication of these viruses and therefore, an antiviral drug target [30]. SARS-CoV-2 M^{pro} is a 33.8-kDa protease with a high homology to that of SARS-CoV (96% sequence identity) [6] as well as other

coronaviruses (41–51% identity and 73–80% similarity). M^{Pro} protein is a homodimer with two monomers oriented perpendicularly to each other (Figure 2a). Each monomer comprises three domains with the first two adopting a chymotrypsin fold for its catalytic activity. The third domain for homo-dimerization has been found to be critical to the catalytic activity [31, 32]. Similarly, the M^{Pro} chymotrypsin fold is similar to other 3C-like proteases from the picornavirus family, such as rhinovirus [33, 34] causing common cold [35–39]. Figure 2 shows the structure of SARS-CoV-2 M^{Pro} in complex with a representative peptidomimetic inhibitor N3 [40], which exemplifies the M^{Pro}-substrate interactions (Figure 2b, c) and mechanism of catalysis that can be used for rational drug design.

M^{Pro} recognizes its substrates with a consensus sequence P2P1-P1' and hydrolyzes the amide bond between P1 and P1', in which the P1 is always Gln, the P1' is Ser or Ala, and the P2 is a hydrophobic Leu, Phe or Val (Figure 2d). Compound N3 occupies all of the substrate binding pockets, closely resembling an M^{Pro} substrate (Figure 2b). The Cys145 -SH group undergoes a Michael addition reaction and forms a covalent bond with the acrylate group of compound N3 (Figure 2c), significantly strengthening its binding. The N3 lactam group mimics Gln (P1) and occupies the S1 pocket composed of Phe140, Leu141, Asn142, Glu166, His163 and His172. The P1 lactam forms multiple hydrogen bonds with Phe140, Glu166 and His163. The P2 Leu sidechain is located in and has hydrophobic interactions with the S2 pocket defined by His41, Met49, Tyr54, Met165 and Asp187. There is also a hydrogen bond between the amide of Leu and Gln189. The side chain of the P3 Val is open to the solvent, while the P4 Ala residue of compound N3 occupies the S4 pocket formed by Met165, Leu167, Phe185, Gln192 and Gln189. The inhibitor terminal oxazole group sitting on the edge of the pocket might have hydrophobic interactions with Pro168, Thr190 and Ala191. The benzyl ester group of the inhibitor is located in the S1' pocket with hydrophobic interactions with Thr24 and Thr25.

Mechanistically, the -SH group of Cys145 is deprotonated by His41 and attacks the carbonyl group of the amide bond between the P1 and P1' residues to form a thioester intermediate (Figure 2e). The protonated His41 also acts as an acid to facilitate the leaving of the P1' amine. The ensuing hydrolysis of the thioester intermediate gives the P1 acid to complete a catalytic cycle.

4. Inhibitors of SARS-CoV and -CoV-2 M^{Pro}

Due to M^{Pro}'s essential roles in viral replication, a number of peptidic, peptidomimetic and non-peptidic small molecule inhibitors of M^{Pro} have been designed, discovered and developed (Supporting Information Table S1). Most of these inhibitors feature an electrophilic “warhead” group, which was designed to react and covalently bind the nucleophilic -SH group of Cys145.

4.1. Peptidic and peptidomimetic inhibitors

4.1.1. Aldehyde-based inhibitors—Representative M^{Pro} inhibitors with an aldehyde “warhead” are shown in Figure 3. Peptidomimetic aldehydes, including compound **11a**, were reported as covalent inhibitors of SARS-CoV-2 M^{Pro} [41]. **11a** demonstrated potent enzymatic activity with an IC₅₀ value of 53 nM and cellular antiviral EC₅₀ value of 530

nM. Its binding structure in SARS-CoV-2 M^{PRO} as well as in vivo pharmacokinetics and toxicities were also studied. Compound **18p** with a phenyl group at the P2 position instead of cyclohexyl group in **11a** also retained the activities [42].

Compound GC373 and its bisulfite adduct prodrug GC376, initially used to treat feline coronavirus, were found to inhibit M^{PRO} [43] with submicromolar IC₅₀ values. These compounds showed strong anti-SARS-CoV-2 activity in cells with EC₅₀ values of 1.5 and 0.92 μM. GC376 was also reported by other groups [44–47] and showed broad-spectrum activity against coronaviruses, including SARS-CoV [48]. However, it showed poor pharmacokinetics and limited in vivo anti-SARS-CoV-2 activity in mice [49, 50]. Modification of GC376 yielded inhibitors with moderately improved enzymatic and cellular activities [51]. Interestingly, deuterated GC-376 showed significantly enhanced potencies in SARS-CoV-2 infected cells and mice [52], despite its similar enzymatic activity to the parent inhibitor. X-ray crystallographic studies also indicated the deuterated GC-376 binds to SARS-CoV-2 M^{PRO} similarly. Compared with GC373/GC376, compounds with different capping groups at the P3 position [53–60], such as compounds **6e** [53] and **2a** [54] also showed similar or better biochemical and cellular antiviral activities. Calpeptin with a *n*-butyl P1 sidechain showed modest activity against SARS-CoV-2 M^{PRO} (IC₅₀ = 10.69 μM) [47], but it exhibited a potent antiviral EC₅₀ of 72 nM in Vero cells [61], presumably due to off-target effects. MPI8/TG-0205221 was found to exhibit dual inhibition of SARS-CoV M^{PRO} (K_i = 53 nM) and human cathepsin L (which is also a cysteine protease critical to the virus entry), with good selectivity over other cathepsins [62, 63]. It showed low-nM antiviral activities together with stabilities in mouse, rat and human plasma [62]. However, despite its increased enzymatic activity, analogous compound MPI3 with smaller hydrophobic P2 and P3 sidechains had no antiviral activity up to 10 μM, possibly due to cellular stability issues [64]. Other similar aldehyde inhibitors were reported [47, 48, 64–74].

M^{PRO} inhibitor MI-09 with an azabicyclo[3.1.0]hexane P2 moiety is one of the most potent inhibitors with an IC₅₀ of 15.2 nM. It showed potent anti-SARS-CoV-2 activities in cell-based assays (EC₅₀ = 0.86 μM) and in a mouse model. MI-09 also possesses good pharmacokinetics [70], e.g., T_{1/2} = 4.53 h. Structurally similar compounds, such as UAWJ9–36-3, were also reported [71, 75]. In another study, a variety of proline derivatives at the P2 were explored, which led to the finding of compound **12** with an IC₅₀ of 5 nM against SARS-CoV-2 M^{PRO} and an antiviral EC₅₀ of 5.3 μM, while it showed a moderate cytotoxicity (CC₅₀ of 28.4 μM) [76].

4.1.2. Ketone-based inhibitors—Although aldehyde-based inhibitors of M^{PRO} have potent enzyme activities, the aldehyde group is chemically reactive and often associated with off-target effects and undesired toxicities. Less electrophilic ketone has been explored as the “warhead” group of M^{PRO} inhibitors (Figure 4).

Benzothiazolyl ketone **5h**/YH-53 was found to be a potent inhibitor of SARS-CoV M^{PRO} (K_i = 6 nM) [77–80] and SARS-CoV-2 M^{PRO} (K_i = 18 nM) with cellular antiviral activities [81]. In addition, it had no cytotoxicity and showed favorable in vivo pharmacokinetics except for a low oral bioavailability [82]. Structurally similar PF-00835231 with a hydroxylmethyl ketone “warhead” retained potent biochemical and antiviral activities (IC₅₀ = 6.9 nM and

EC₅₀ = 231 nM) with more favorable drug properties [83–86]. Phase I clinical trials (NCT04627532 and NCT04535167) of its phosphate prodrug PF-07304814 have been completed, showing good safety profiles [84, 85]. Moreover, in a comparison study, the hydroxymethyl ketone-based inhibitor was found to exhibit more biochemical activity against SARS-CoV-2 M^{PRO} than does structurally similar, nitrile-based nirmatrelvir [87].

Heteroaromatic and aliphatic α -acyloxymethyl ketone warheads were found in a series of SARS-CoV-2 M^{PRO} inhibitors, such as compound **15l** showing biochemical IC₅₀ of 19 nM and cellular antiviral EC₅₀ of 300 nM without overt cytotoxicity [88]. A similar phenyl α -acyloxymethylketone compound was also reported with weak activities as well as poor protease selectivity [89].

α -Ketoamide compounds were reported to be M^{PRO} inhibitors [32, 90]. Compound **11r** exhibited an IC₅₀ of 0.71 μ M against SARS-CoV M^{PRO} and inhibited the viral replication in Vero cells with an EC₅₀ of 2.1 μ M [90]. Incorporation of P3-P2 amide bond of **11r** into a pyridone ring led to the discovery of **13b** with good drug-like properties, although its enzymatic and cellular activities were slightly compromised [32]. A subsequent study indicated that one diastereomer (**13b-K**) of **13b** with a *S*-P2 moiety is a more potent inhibitor with an IC₅₀ of 0.12 μ M, but the corresponding *R*-enantiomer is almost inactive (IC₅₀ > 5 μ M) [91]. **13b-K** had more potent anti-SARS-CoV-2 activity with EC₅₀s of 0.84–3.4 μ M. Calpain inhibitor XII with a *n*-propyl P1 sidechain showed potent inhibition of SARS-CoV-2 M^{PRO} as well as a broad spectrum of anti-coronavirus activities including SARS-CoV and -CoV-2 [47, 48]. Anti-hepatitis C virus drug boceprevir with a cyclobutylmethyl P1 moiety was found to be an inhibitor of SARS-CoV-2 M^{PRO} with IC₅₀ values ranging from 0.95 μ M to 8.0 μ M by several research groups [44, 47, 92–96]. It also exhibited broad anti-coronavirus activities including SARS-CoV-2 (EC₅₀ = 1.3–19.6 μ M) [44, 47, 48, 92]. With a 5-membered lactam at the P1 position that mimics Gln, structurally similar ML1000 showed significantly increased potencies (IC₅₀ = 12 nM and EC₅₀ = 100 nM) [97]. However, naltaprevir with a *n*-butyl P1 showed similar activities to boceprevir [47, 92, 95, 98]. SY110, obtained from compound screening followed by structural modification, exhibited strong inhibition against SARS-CoV-2 M^{PRO} with an IC₅₀ of 14.4 nM and broad anti-coronavirus activity including different variants of SARS-CoV-2 and SARS-CoV with EC₅₀s in sub- μ M to low μ M range [99]. With favorable pharmacokinetic properties and safety profiles, oral administration of SY110 significantly protected mice infected with SARS-CoV-2 (Omicron strain).

Compound Y180, having a methyl ketone “warhead” group, was reported to be a potent SARS-CoV-2 M^{PRO} inhibitor (IC₅₀ = 8.1 nM) with advanced preclinical studies. It exhibited excellent antiviral activities against wild-type and mutant SARS-CoV-2 with EC₅₀s of 11.4–34.4 nM [100]. With good oral bioavailability (92.9% in mice), pharmacokinetics (e.g., *T*_{1/2} = 1.42 h) and no overt toxicities, Y180 showed strong anti-SRAS-CoV-2 activities in several animal models. Other M^{PRO} inhibitors with a phthalhydrazido, or trifluoromethyl-ketone were also reported with low or untested antiviral activities [77, 101–103].

4.1.3. α , β -Unsaturated esters and related Michael acceptors— α , β -Unsaturated ester, amide and related groups can covalently bind Cys145 through a Michael addition

reaction and is therefore a good “warhead” group for cysteine proteases. Representative inhibitors are shown in Figure 5. Rupintrivir (AG7088), a potent inhibitor of rhinovirus 3CL^{pro}, was found to have negligible inhibitory activities against M^{pro} of SARS-CoV and -CoV-2 (IC₅₀ >= 68 μM) [30, 104–106], but it strongly inhibited replication of SARS-CoV-2 with an EC₅₀ of 1.87 μM [107]. Compound **18c** with a cinnamoyl P3 moiety showed good inhibitory activities against SARS-CoV M^{pro} (IC₅₀ = 1 μM) as well as cellular viral replication (EC₅₀ = 0.18 μM) without overt toxicity [105].

Structure-based drug design led to the discovery of SARS-CoV M^{pro} inhibitor N3 (Figure 2b) with a *K_i* of 9.0 μM [108]. It is also an inhibitor against SARS-CoV-2 M^{pro} as well as the virus replication with an EC₅₀ of 16.77 μM [40]. TG-0203770, with a 1-(*tert*-butoxy)ethyl moiety at P3, is a potent inhibitor of SARS-CoV and -CoV-2 M^{pro} (*K_i* = 58 and 151 nM) [109] with a strong cellular anti-SARS-CoV-2 EC₅₀ of 2.88 μM [45]. SM141 with a benzyl group at the P2 and P3 showed dual inhibition of SARS-CoV-2 M^{pro} and human Cathepsin L with IC₅₀ of 0.9 μM and 60 nM, respectively [110]. It potently inhibited cellular replication of SARS-CoV-2 with an EC₅₀ of 8.2 nM without cytotoxicity. It can significantly reduce viral loads and prolong animal survivals in SARS-CoV-2-infected mice. Other α, β-unsaturated ester-based and related inhibitors of SARS-CoV and -CoV-2 M^{pro} were also reported [109, 111–114], among which SPR39 with a vinyl methyl ketone Michael acceptor showed strong SARS-CoV-2 M^{pro} inhibition with a *K_i* of 0.252 μM and an antiviral EC₅₀ of 1.5 μM [114].

Similarly, acrylamide or vinyl sulfone could undergo a Michael addition reaction and be a potential warhead. Acrylamide compound MPI80 was reported to potently inhibit SARS-CoV-2 M^{pro} with an IC₅₀ of 34 nM. It blocked cellular viral replication with an EC₅₀ of 0.70 μM [115]. Several other acrylamide- [116] or vinyl sulfone-based inhibitors of SARS-CoV-2 M^{pro} [117, 118] were also reported with low or untested antiviral activities.

4.1.4. Haloacetyl-based inhibitors—Compound screening identified a chloroacetamide compound JCP400 (Figure 6) to be an inhibitor of SARS-CoV-2 M^{pro} with an IC₅₀ of 1.74 μM as well as moderate antiviral activities [89]. But it had similar activities against other proteases, such as cathepsins L and B, showing a poor selectivity. Jun9–62-2R with a dichloroacetamide group was developed as a covalent inhibitor of SARS-CoV and -CoV-2 M^{pro}, showing biochemical IC₅₀ and cellular antiviral EC₅₀ in sub- to low-μM range [119]. Azapeptidic compounds bearing a mono- or di-chloroacetamide, such as MPI89, were reported to be a potent SARS-CoV-2 M^{pro} inhibitor [115]. MPI89 exhibited potent antiviral activities with low cytotoxicity, but it had a short half-life in plasma (~ 20 min). Compound **29** was discovered as a covalent inhibitor of SARS-CoV-2 M^{pro} with an IC₅₀ of 1.72 μM [120], but it showed more potent inhibitory activity against SARS-CoV-2 PL^{pro} (IC₅₀ = 0.67 μM). Compound **29** was found to inhibit replication of a variety of SARS-CoV-2 strains in Vero cells with EC₅₀s of 0.32–1.37 μM. Other haloacetyl-based inhibitors were also reported [117, 121–124], among which several compounds showed potent biochemical inhibition, but none of them were tested in cells or animals [117, 122, 123].

4.1.5. Nitrile-based inhibitors—Modifications of hydroxymethyl ketone-based inhibitor PF-00835231 (Figure 4) led to the discovery of M^{pro} inhibitor nirmatrelvir

(initially coded as PF-07321332) with a nitrile “warhead” (Figure 6). nirmatrelvir showed a highly potent activity ($K_i = 3.11$ nM) against SARS-CoV-2 M^{PRO}. While it is less active than PF-00835231 ($K_i = 0.27$ nM), nirmatrelvir exhibited ~3× more cellular antiviral activities [86]. Oral administration of nirmatrelvir significantly reduced the viral loads in SARS-CoV-2 infected mice and protected them from weight losses [86]. Furthermore, immunohistochemical analysis also revealed it significantly alleviated virus-caused lung damages in a dose-dependent manner. Nirmatrelvir exhibited a good safety profile with a high selectivity over a broad panel of human proteins. It is also negative in the genetic toxicity studies and rat micronucleus assay. Furthermore, the embryo-fetal, fertility and early embryonic development studies indicated nirmatrelvir is a safe drug in animal models [125]. Other nirmatrelvir analogs with the same P1, P2 and P3 were also reported [126].

Another nitrile compound **18b** (Figure 6) with an indole P3 moiety showed potent biochemical activity and strong antiviral activity against SARS-CoV-2, together with a good selectivity over human cysteine proteases [127]. In addition, nitrile-based peptidomimetic compound Cbz-AVLQ-CN, designed based on the autocleavage tetrapeptide sequence of SARS-CoV M^{PRO}, was found to have an IC₅₀ of 4.6 μM as well as a broad inhibitory activities against other coronavirus M^{PRO} with IC₅₀s of 1.3–4.6 μM [128, 129]. Compound screening followed by medicinal chemistry studies identified azanitrile compound Gü3619 (Figure 6) as a potent irreversible covalent inhibitor of SARS-CoV-2 M^{PRO} with an IC₅₀ of 37.8 nM, but it also potently inhibited human cathepsins L and B [130].

4.1.6. Other miscellaneous compounds—Epoxy ketone compound WRR183 (Figure 7) was found to inhibit SARS-CoV M^{PRO} with a K_i of 2.2 μM and the virus replication with an EC₅₀ of 12 μM [131]. Its electrophilic epoxy β-carbon atom forms a thioether bond with M^{PRO} Cys145. Several substrate-based oligomeric peptides or peptidomimetic compounds were reported to be inhibitors of SAR-CoV and/or -CoV-2 M^{PRO} with sub-μM activities [132–140].

Virtual screening followed by medicinal chemistry led to the discovery of non-covalent inhibitor ML188 (Figure 7) with IC₅₀s in the low μM range against SARS-CoV and -CoV-2 M^{PRO} [141, 142]. In the cell-based assay, ML188 exhibited anti-SARS-CoV activity with an EC₅₀ value of 13 μM. Modification of ML188 yielded more potent inhibitor 23R (Figure 7) [143].

Anti-HIV drug atazanavir, an inhibitor of HIV-1 (aspartic) protease, was found to inhibit SARS-CoV-2 M^{PRO} as well as cellular viral replication in the sub-μM to μM range [144, 145]. It also exhibited significant anti-SARS-CoV-2 activity in mice [145]. Cobicistat, an inhibitor of human cytochrome P450 and an adjuvant drug for HIV treatment, was reported to be a SARS-CoV-2 M^{PRO} inhibitor with an IC₅₀ of 6.7 μM [107, 146]. However, inhibition of SARS-CoV-2 M^{PRO} by these two drugs were not confirmed by other researchers [65, 147]. In addition, immune-modulating polypeptide drug glatiramer acetate was also identified to be a weak SARS-CoV-2 M^{PRO} inhibitor with mild antiviral activity [148].

4.2. Non-peptidic small molecule inhibitors

Non-peptidic inhibitors of SARS-CoV and -CoV-2 M^{pro} have been discovered and developed, with the majority initially identified from compound screening including virtual screening.

4.2.1. Flavonoids—Natural flavonoid compound baicalin (Figure 8) was identified as an inhibitor of SARS-CoV-2 M^{pro} with an IC₅₀ of 6.41 μM, which inhibited replication of SARS-CoV-2 in cells (EC₅₀ = 27.87 μM) [149, 150]. Baicalein, the parent compound of baicalin, exerted improved biochemical and cellular activities against SARS-CoV and -CoV-2 [149–151]. Analogs with more hydroxyl groups in the 2-phenyl substituent of baicalein, such as myricetin, retained the biochemical activity [152, 153]. Interestingly, myricetin was found to be oxidized by O₂ to become a quinone and covalently bind to Cys145 of SARS-CoV-2 M^{pro} (Figure 18g, h) [152]. However, flavonoid compounds without the 2-phenyl substitution, such as esculetin-4-carboxylic acid ethyl ester, is a weak SARS-CoV M^{pro} inhibitor [154]. Other flavonoids and related analogs have also been reported to inhibit M^{pro} with low-μM IC₅₀ values [151, 155–171], while their antiviral activities were not disclosed.

4.2.2. Quinoline analogs—Quinoline compound MAT-POS-e194df51-1 (Figure 9) was identified in an X-ray-based fragment screening campaign to be a potent SARS-CoV-2 M^{pro} inhibitor (IC₅₀ = 36.8 nM), which exhibited potent anti-SARS-CoV-2 activities with EC₅₀ as low as 63.8 nM [172]. It had acceptable in vivo pharmacokinetic and toxicities (e.g., T_{1/2} = 1.4 h in rats) with oral bioavailability (18% in rats). Quinoline compound DA-3003-1 showed an inhibitory IC₅₀ of 2.63 μM against SARS-CoV-2 M^{pro} and an EC₅₀ of 4.47 μM in the SARS-CoV-2 cytopathic effect (CPE) assay, but it is cytotoxic (CC₅₀ = 7.74 μM) [173]. Compound **19** was discovered from virtual screening followed by structure-based optimization, having an IC₅₀ of 77 nM against SARS-CoV-2 M^{pro} as well as antiviral EC₅₀ values as low as 77 nM [174]. Compound **C7**, from structure-based drug development based on baicalein (Figure 8), exhibited a potent activity against SARS-CoV-2 M^{pro} (IC₅₀ = 85 nM) and cellular viral replication (EC₅₀ = 1.10 μM) [175].

Several quinolone or related drugs were reported to inhibit M^{pro} of SARS-CoV and -CoV-2. Anti-hepatitis C virus (HCV) drug simeprevir, an inhibitor of HCV NS3/4A (serine) protease, inhibited SARS-CoV-2 M^{pro} with IC₅₀ of 2.46–13.74 μM [47, 176, 177], while it also showed comparable activities against SARS-CoV-2 RNA-dependent RNA polymerase (RdRp) (IC₅₀ = 5.5 μM) [177]. Simeprevir inhibited replication of SARS-CoV-2 in Vero cells with an EC₅₀ of 1.40 μM [176]. Nelfinavir, a HIV-1 protease inhibitor, was reported to only partially inhibit SARS-CoV M^{pro}. It can inhibit cellular replication of SARS-CoV and -CoV-2 with EC₅₀ values of 0.048–3.3 μM by several groups [107, 178–180]. However, nelfinavir was found to not inhibit M^{pro} by another laboratory [65]. Also, nelfinavir was unable to inhibit SARS-CoV-2 replication in hamsters [181]. Pelitinib, an anticancer drug inhibiting human epidermal growth factor receptor (EGFR), was found to bind to an allosteric site of SARS-CoV-2 M^{pro}. Although it inhibited proliferation of SARS-CoV-2 in Vero E6 cells with an EC₅₀ of 1.25 μM, its biochemical activity against M^{pro} was not disclosed [61].

Compound screening or rational drug design led to discovery and development of other quinoline analogs [65, 182–194], with the best compounds showing strong inhibition of M^{Pro} [185, 186, 188, 193]. But their cellular anti-SARS-CoV-2 activities were not evaluated or weak.

4.2.3. Terpenoids—Bardoxolone methyl (Figure 10) was identified as a SARS-CoV-2 M^{Pro} covalent inhibitor through screening of compounds bearing an electrophilic group [195]. With a moderate enzyme activity (IC₅₀ = 5.81 μM), it showed potent cellular antiviral activity (EC₅₀ = 0.29 μM). A cell-based M^{Pro} inhibitor screening yielded hydroxyprogesterone (cellular IC₅₀ of 2.47 μM), which blocked replication of SAR-CoV-2 in Vero cells with an EC₅₀ of 2.77 μM [176]. The *S*-enantiomer of phloroglucinol terpenoid **3** was identified to be an inhibitor of SARS-CoV-2 M^{Pro} from virtual screening with an IC₅₀ of 7.5 μM and antiviral EC₅₀ of 4.5 μM, while its *R*-isomer was less active [196]. Several other terpenoid compounds, including betulinic acid, were found to inhibit SARS-CoV and -CoV-2 M^{Pro} with micromolar IC₅₀ values [197–203].

4.2.4. Pyridinyl ester and related compounds—Activated esters that could covalently bind to Cys145, including pyridinyl esters [45, 81, 130, 204–207], benzotriazole esters [208], and their analogs [209–212], were explored as SARS-CoV and -CoV-2 M^{Pro} inhibitors. Pyridinyl ester compound GRL-0920 (Figure 11) was found to be a potent inhibitor of SARS-CoV M^{Pro} with an IC₅₀ of 30 nM, which blocked the cellular viral replication with an EC₅₀ of 6.9 μM [204]. It also showed comparable activities against SARS-CoV-2 M^{Pro} and replication [205, 206]. Other analogs of GRL-0920 were developed with similar or reduced activities [81, 205, 206]. Mechanistically, the -SH group of Cys145 nucleophilically attacks and hydrolyzes the activated ester, with the 5-chloropyridin-3-yl being a good leaving group. The thioester product has been confirmed by X-ray crystallography and mass spectrometry studies [205, 206]. Several other pyridyl esters or their analogs were also found to be M^{Pro} inhibitors [45, 130, 207, 212, 213], including WNN2048-F004 (IC₅₀ = 103.1 nM). However, it only showed modest cellular antiviral activity against SARS-CoV-2.

A series of thioesters were reported, including compound **3w** with IC₅₀s of 61.3 and 11.4 nM against SARS-CoV and -CoV-2 M^{Pro} [214]. It showed an EC₅₀ of 0.11 μM against the replication of SARS-CoV-2 virus without cytotoxicity up to 10 μM. In addition, benzotriazole esters were reported as irreversible SARS-CoV M^{Pro} inhibitors [208]. The most potent compound **8** (Figure 11) showed potent inhibition of M^{Pro} with a *K_i* of 7.5 nM, while no cellular antiviral activities were disclosed. X-ray crystallography and mechanistic studies revealed that these inhibitors acylate the active site Cys145 with their benzotriazole being as a leaving group [215]. Moreover, dithiocarbamate compound **1**, identified from high-throughput screening (HTS), potently inhibited M^{Pro} of SAR-CoV-2 (IC₅₀ = 21 nM), SARS-CoV (IC₅₀ = 383 nM) and other coronaviruses. It covalently modifies Cys145 to form a dithiocarbamate adduct. Compound **1** was found to inhibit cellular proliferation of SARS-CoV-2 with an EC₅₀ of 1.06 μM [216].

4.2.5. Ebselen analogs—Through high-throughput screening, selenium-containing compound ebselen (Figure 11) was found to be an M^{Pro} inhibitor with an IC₅₀ of 0.67 μM,

which inhibited cellular replication of SARS-CoV-2 with an EC₅₀ value of 4.67 μM [40]. It was later reported to be a nonspecific inhibitor [65, 217, 218]. Modification of ebselen has yielded several more potent inhibitors of SARS-CoV-2 M^{PRO} [219–227], including MR6–18-4 with an IC₅₀ of 0.35 μM as well as cellular anti-SARS-CoV-2 EC₅₀ of 3.74 μM. An X-ray crystallographic study suggested that ebselen (and its analog) covalently modifies the Cys145 -SH group of SARS-CoV-2 M^{PRO} by forming a S-Se bond, while other atoms of ebselen cannot be found in the structure [220].

4.2.6. Benzotriazole-based inhibitors—Benzotriazole compound ML300 (Figure 12) was identified as a SARS-CoV-2 M^{PRO} inhibitor with an IC₅₀ value of 4.99 μM through compound screening followed by structure-based medicinal chemistry [228, 229]. Modest antiviral activity in cells (EC₅₀ = 19.90 μM) was observed. Further modification of ML300 led to a more potent inhibitor CCF0058981 with an IC₅₀ of 68 nM as well as an EC₅₀ of 497 nM against SARS-CoV-2 [229].

4.2.7. Pyrimidine analogs—High-throughput screen identified pyrimidine compound carmofur to be an inhibitor of SARS-CoV-2 M^{PRO} (IC₅₀ = 1.82 μM) [40], which modestly inhibited cellular replication of SARS-CoV-2 [230]. The structure of SARS-CoV-2 M^{PRO} in complex with carmofur was determined [230]. Subsequent studies revealed that carmofur is a nonspecific inhibitor, and it also showed sub-μM activities against SARS-CoV-2 PL^{PRO} and other 3CL^{PRO} [65, 217]. Another pyrimidine-containing compound **23** was discovered as a potent SARS-CoV-2 M^{PRO} inhibitor with an IC₅₀ of 20 nM, using virtual screening [231, 232]. Compound **23** was able to inhibit cellular SARS-CoV-2 proliferation with an EC₅₀ of 0.84 μM. Its derivative compound **19** showed significantly increased antiviral activity against SARS-CoV-2 (EC₅₀ = 80 nM) [233]. Several other pyrimidine and related compounds were also identified to be M^{PRO} inhibitors with low-μM IC₅₀s [166, 207, 234–237].

4.2.8. Acrylamide and related compounds—Through screening DNA-encoded compound libraries, compound **1e** with an acrylamide group (Figure 13) was identified as a novel covalent inhibitor of SARS-CoV and -CoV-2 M^{PRO} (IC₅₀ = 3.5 and 2.0 μM) [238]. However, it showed only weak anti-SARS-CoV-2 activity in cells with an EC₅₀ of 33 μM. In addition, LY1 was found to be a dual inhibitor of SARS-CoV-2 M^{PRO} (IC₅₀ = 0.12 μM) and PL^{PRO} (IC₅₀ = 0.99 μM) [239]. It can inhibit the viral proliferation with an EC₅₀ of 3.9 μM. Several other non-peptidic acrylamide- [240, 241], chloroacetamide- [242] and vinyl sulfonamide-based [243] covalent inhibitors of SARS-CoV and SARS-CoV-2 M^{PRO} were also reported with low or untested antiviral activities.

4.2.9. Isatin analogs—Isatin compounds were previously found to be potent inhibitors of related rhinovirus 3CL^{PRO} [244], with its keto group forming a covalent bond with the active site cysteine residue. Isatin compounds were evaluated for their ability to inhibit M^{PRO} [245–248]. Compounds **4o** and **5f** (Figure 13) showed strong inhibition of SARS-CoV M^{PRO} with IC₅₀s of 0.95 and 0.37 μM, respectively [245, 246]. Recently, isatin compound **5f** was found to inhibit SARS-CoV-2 M^{PRO} (IC₅₀ = 45 nM) [248]. No cellular antiviral activities of these compounds were reported. Given the similarities between rhinovirus 3CL^{PRO} and M^{PRO}, these isatin inhibitors of M^{PRO} might covalently bind to Cys145.

4.2.10. Metal-containing inhibitors—Transition metal complexes were reported to potently inhibit SARS-CoV and SARS-CoV-2 M^{Pro}, including 1-hydroxypyridine-2-thione zinc, bis(*L*-aspartato-*N,O*) zinc(II) ethanate (JMF1586), thimerosal and phenylmercuric acetate, auranofin, and Re(I) tricarbonyl complex (Figure 14) [249–255]. X-ray crystallographic studies showed that His41 and C145, the catalytic dyad of M^{Pro}, chelate Zn²⁺ of JMF1586 [250]. Mechanism of inhibition of other transition metal complexes could similarly involve the formation of a coordination bond(s) with Cys145 and/or His41. No cellular antiviral activities of these compounds were reported.

4.2.11. Triazine compounds—Trisubstituted triazine compound S-217622 (Figure 15), a non-covalent, potent inhibitor of SARS-CoV-2 M^{Pro} (IC₅₀ = 13 nM), was discovered from virtual screening followed by medicinal chemistry optimization [256]. It selectively inhibited SARS-CoV-2 M^{Pro} over the human proteases. S-217622 showed potent antiviral activities in Vero cells against various strains of SARS-CoV-2 with EC₅₀ values of 0.29–0.50 μM. Oral administration of S-217622 significantly reduced the titers of SARS-CoV-2 in mice. It also possesses a good pharmacokinetic profile with *T*_{1/2} of 2.4 h and a high oral bioavailability of 96.7% in rats, as well as a good safety profile in clinical trials [257]. S-217622, renamed to be ensitrelvir, has been approved in Japan to treat COVID-19.

4.2.12. Other miscellaneous compounds—Other miscellaneous compounds were identified as M^{Pro} inhibitors. Trisubstituted piperazine compound GC-14 was found to be a SARS-CoV-2 M^{Pro} inhibitor with an IC₅₀ of 0.40 μM as well as a high selectivity over human cysteine proteases [258]. It suppressed replication of SARS-CoV-2 in Vero cells with an EC₅₀ of 1.1 μM without cytotoxicity. Replacement of the nicotinoyl group in GC-14 with a chloroacetyl group yielded the covalent inhibitor GD-9 with a 2-fold increase in enzyme inhibition, but it showed a ~2-fold decreased antiviral activity together with significant cytotoxicity [259]. 1,4-Naphthoquinone compound **15** was found to potently inhibit SARS-CoV-2 M^{Pro} (IC₅₀ = 72 nM) but moderately blocked the viral replication in Vero cells (EC₅₀ = 4.55 μM) [260].

Screening of a DNA-encoded library yielded compound CDD-1976 as a potent SARS-CoV-2 M^{Pro} inhibitor with a *K*_i of 37 nM, which inhibited the virus replication with an EC₅₀ of 2.50 μM [261]. Compound ALG-097111 was reported to be a potent SARS-CoV-2 M^{Pro} inhibitor with an IC₅₀ of 7 nM as well as a high selectivity over cathepsin L [262]. It showed significant cellular (EC₅₀ = 200 nM) and in vivo antiviral activity against SARS-CoV-2. However, the structure of ALG-097111 has not been disclosed. From virtual screening, compounds Z1244904919 and Z1759961356 were found to be inhibitors of SARS-CoV-2 M^{Pro} (IC₅₀ = 0.73 and 0.69 μM), which suppressed the viral replication in Vero cells with EC₅₀s of 4.98 and 8.52 μM, respectively [263]. Walrycin B, a strong inhibition against SARS-CoV-2 M^{Pro} (IC₅₀ = 0.26 μM), demonstrated an EC₅₀ of 3.55 μM against SARS-CoV-2 replication in Vero cells, but it showed a high cytotoxicity (CC₅₀ = 4.25 μM) [173].

Several FDA-approved drugs were found to be SARS-CoV and/or -CoV-2 M^{Pro} inhibitors. Tyrosine-kinase inhibitor masitinib (Figure 16), an anticancer drug, inhibited SARS-CoV-2 M^{Pro} (IC₅₀ = 2.5 μM) and the viral replication (EC₅₀ = 3.2 μM) [264]. Oral administration of masitinib significantly reduced the viral loads in the lungs and noses and prolonged

the survivals of SARS-CoV-2 infected mice. Phosphodiesterase inhibitor dipyridamole (an antiplatelet drug) [186], BCL-2 inhibitor venetoclax (an anticancer drug) [176], and cinacalcet (a hypercalcemia drug targeting calcium sensing receptor) [176] were also reported to inhibit SARS-CoV-2 M^{Pro} with IC₅₀s of 0.60, 3.18, and 5.99 μM, while they showed more potent cellular antiviral activities (EC₅₀ = 0.1, 1.18, and 2.93 μM). Interestingly, dipyridamole was used in the clinic to treat severely ill COVID-19 patients [265]. Manidipine (an antihypertension drug) was reported to be an inhibitor of SARS-CoV-2 M^{Pro} with an IC₅₀ of ~5 μM [93]. But other researchers found that manidipine had only weak or no inhibitory activity [65, 266].

Some other compounds were reported to inhibit SARS-CoV and/or -CoV-2 M^{Pro}, but their antiviral activities were weak or unreported [40, 47, 65, 106, 134, 138, 141, 160, 163, 166, 173, 183, 197, 206, 209, 217, 218, 226, 249, 251, 266–318].

5. M^{Pro}-inhibitor interactions

More than 100 crystal structures of M^{Pro} in complex with its inhibitors have been determined with most of them binding to the active site. Upon complexation with these active-site inhibitors, the overall structure of M^{Pro} is little changed. M^{Pro} interactions with three representative covalent peptidomimetic inhibitor are shown in Figure 17, which could facilitate future rational inhibitor design.

Compound **11a** (Figure 3), an aldehyde-based inhibitor, binds to the substrate-binding pocket of SARS-CoV-2 M^{Pro}, with the aldehyde group forming a covalent bond with Cys145 (Figure 17a, b) [41]. The binding is further stabilized by a network of hydrogen bonds between the newly formed hydroxyl group and the “oxyanion hole” residues Cys145, Gly143, Thr26 and Asn142. There are hydrophobic interactions and a hydrogen bond interaction between the backbone of **11a** and His164. The γ-lactam P1 moiety mimics the substrate glutamine side chain and is located in the S1 pocket of M^{Pro} with favorable hydrophobic interactions and hydrogen bonds with Phe140 and Glu166. The cyclohexyl group of the inhibitor fits snugly into the S2 pocket surrounded by Met49, Tyr54, Met165, Asp187, Arg188, and His41. The indole fragment has favorable hydrophobic as well as hydrogen bond interactions with Pro168, Gln189 and Glu166.

Ketone-based peptidomimetic inhibitor **13b** (Figure 4) forms a covalent bond with Cys145 to produce a thiohemiketal (Figure 17c, d), with its hydroxyl group stabilized by a hydrogen bond with His41 [32]. The benzyl amide moiety occupies the S1' pocket with favorable hydrophobic and hydrogen bond interactions with Gly143, Ser144 and Cys145. The P1 γ-lactam is similarly in the S1 pocket of M^{Pro} with favorable hydrophobic and hydrogen bonds with Phe140, Glu166 and His163. The cyclopropylmethyl side chain of the inhibitor occupies the S2 pocket, while the pyridone moiety resembles the binding of the substrate backbone, forming hydrogen bonds with Glu166. Although the terminal *tert*-butyloxycarbonyl (Boc) group does not fit nicely in the S4 pocket, its interactions with the protein contribute to the binding of compound **13b**, as removal of the Boc group significantly reduced the inhibitory activity [32].

Nirmatreivir/PF-07321332 is a nitrile-based inhibitor of M^{Pro} (Figure 6), with its nitrile group covalently binding to Cys145 and forming a thioimidate adduct (Figure 17e, f) [86]. Similarly, its γ -lactam moiety fits well in the S1 pocket with favorable hydrophobic and hydrogen bond interactions with His163, Phe140 and Glu166. The 6,6-dimethyl-3-azabicyclo[3.1.0]hexane moiety is located in the S2 pocket of M^{Pro}, with mostly hydrophobic interactions with Met49, His41, and Asp187. The tri-fluoroacetamide group, along with the *tert*-butyl side chain, occupies the S4 pocket with favorable hydrophobic interactions with Gln189, Met165, and Pro168.

Protein-inhibitor interactions of four representative non-peptidic inhibitors of M^{Pro} are shown in Figure 18. Compound 23R (Figure 7) is a potent, non-covalent inhibitor of M^{Pro} (Figure 18a, b) [143]. Its furan-carboxyl moiety is located in the S1' pocket of M^{Pro} with both hydrophobic and hydrogen bond interactions. The 3-pyridine ring occupies the S1 pocket with favorable hydrophobic interactions as well as hydrogen bonds with His163 and Ser144. The biphenyl moiety fits nicely into the S2 pocket with hydrophobic and π - π stacking interactions. There is another hydrogen bond between the other amide oxygen of the inhibitor and Glu166. The chiral α -methylbenzyl group is extended into the S4 pocket of M^{Pro} with mostly hydrophobic interactions.

S-217622 (Figure 15) is a potent, non-covalent inhibitor of M^{Pro} [256]. The 1-methyl-1*H*-1,2,4-triazole group of S-217622 occupies the S1 pocket with favorable hydrophobic and hydrogen bond interactions with Ser144, His163 and Asn142 (Figure 18c, d). Its central triazine-2,4-dione core resides on a shallow platform linking the S1 and S2 pockets, forming a network of direct or water-mediated hydrogen bonds with Asn142, Ser144, Cys145, and Glu166. There might be also favorable hydrophobic or other interactions between the aromatic ring and the -SH of Cys145 (with the distance of ~ 5 Å). The 2,4,5-trifluorobenzyl substituent fits well in the S2 pocket with favorable hydrophobic and π - π stacking (with His41) interactions. The indazole moiety of S-217622 is situated in the S1' pocket with stabilizing hydrophobic as well as hydrogen bond interactions with Thr26. The -NH- linker group interacts with His41 and Gln189 through water-mediated hydrogen bonds. Furthermore, this fragment may establish hydrophobic interactions with Met49 and Thr25.

Masitinib (Figure 16) is a moderate, non-covalent inhibitor SARS-CoV-2 M^{Pro}, with its long, linear body binding across the S1 and S2 pockets of the protein (Figure 18e, f) [264]. Its thiazole-pyridine moiety is located the S1 pocket with hydrophobic interactions as well as a hydrogen bond with His163. The -NH- linker group forms a hydrogen bond with His164. The toluene fragment is situated in the S2 pocket of M^{Pro} with hydrophobic and π - π stacking (with His41) interactions. Its benzamide and terminal *N*-methylpiperazine moieties protrude from the S2 pocket further into the protein, with mostly hydrophobic interactions as well as hydrogen bonds with His41 and Thr24.

Natural flavonoid compound myricetin (Figure 8) was found to be oxidized by O₂ to become an *ortho*-quinone, which is a covalent inhibitor of SARS-CoV-2 M^{Pro} with a unique binding mode (Figure 18g, h) [152]. The *ortho*-quinone acts as an electrophile and forms a covalent bond with Cys145. The molecule is mainly located in the S1' and S2 pockets.

The hydroxyl (or its oxidized form) groups in the pyrogallol fragment form multiple hydrogen bond interactions with Thr26 and Cys145. The pyrogallol ring might also have hydrophobic interactions with Leu27, Asn28, Asn142, Gly143 and Ser144. In addition, the hydroxyl-substituted chromone moiety has hydrogen bond interactions with Gln189 and His164. There are also favorable π - π stacking and hydrophobic interactions between the chromone core and His41, Met165, Asp187 and Arg188.

6. M^{PRO} inhibitors that are FDA-approved or in clinical trials

Nirmatrelvir in combination with ritonavir (brand name Paxlovid) has been approved by FDA for the treatment of mild-to-moderate SARS-CoV-2 infected patients. This clinical trial (NCT04960202) included 2246 adult patients (1120 treated and 1126 controls) with confirmed SARS-CoV-2 infection within 5 days. Treatment with Paxlovid lowered the risk of progression to severe diseases by 89% without obvious safety issues [319]. A large retrospective study including 180,351 high-risk COVID-19 patients revealed that treatment with Paxlovid showed high efficacies in reducing hospitalization and mortality [320]. Another anti-SARS-CoV-2 drug, ensitrelvir fumaric acid (brand name Xocova), has been granted emergency regulatory approval in Japan. As shown in Table 1, a handful of other M^{PRO} inhibitors (including several with their structures undisclosed) have been in different stages of clinical trials (data from clinicaltrials.gov).

7. Conclusion and perspectives

The Covid-19 pandemic caused by SARS-CoV-2 has been an unprecedented catastrophe of the global health in modern history with millions of mortalities and morbidities. It has also resulted in enormous economic losses worldwide. Thanks to expedited development and deployment of effective vaccines and antiviral drugs against SARS-CoV-2, the pandemic has been largely over within 3 years. However, with continuous viral evolution as well as possible emergence of a new coronavirus, drug discovery targeting SARS-CoV-2 and related viruses is needed.

M^{PRO} is a validated drug target for the coronavirus family because of its essential role in the life cycle of coronaviruses. M^{PRO} is a highly conserved protein during evolution [321], which renders a high likelihood of developing a broadly active anti-coronavirus drug or expediting drug discovery against other coronaviruses. Different from the vaccines targeting the spike protein (with frequent mutations), Paxlovid has retained effectiveness against the original to the recent Omicron strains of SARS-CoV-2 [321]. However, treatment with an M^{PRO} inhibitor may pose a selective pressure to generate drug resistance, as recently observed nirmatrelvir-resistant strains of SARS-CoV-2 [322]. Therefore, continued research and development on M^{PRO} inhibition are warranted. Indeed, the rapid development of nirmatrelvir within 2 years has been based on a lead compound against M^{PRO} of SARS-CoV identified in 2003 [323].

This article represents a comprehensive review of small molecule inhibitors of SARS-CoV and -CoV-2 M^{PRO} since 2003. Currently, the highly potent inhibitors are mostly peptidic/peptidomimetic compounds with an electrophilic “warhead” to covalently bind Cys145.

Aldehyde and chloroacetamide group exhibit a high chemical reactivity, but they are often associated with non-specific binding, off-target effects and cytotoxicity. With a reduced and tunable reactivity, ketone, epoxide and Michael acceptor groups represent a balanced choice for the warhead and have been successfully utilized in numerous drugs, such as telaprevir, carfilzomib and neratinib. Due to its weak reactivity, nitrile has been rarely used for this application, but it generally possesses improved chemical and metabolic stabilities as well as target specificity, which are critical for clinical use. As for the main body of the inhibitor, M^{Pro}'s substrate sequence as well as its X-ray structures can be used to guide peptidic/peptidomimetic inhibitor design and facilitate optimization of the activity and selectivity. Non-peptidic inhibitors were mostly from compound screening, with fewer compounds having potent biochemical and antiviral activities. Since non-peptidic compounds tend to resist enzyme-mediated hydrolysis with improved pharmacokinetics, more work on developing non-peptidomimetic M^{Pro} inhibitors is desirable.

In addition, other technologies could be explored to counteract M^{Pro}. Proteolysis-targeting chimera (PROTAC) technology [324] has been developed for target protein degradation, which complements and is often similar to protein inhibition. Several PROTAC molecules with antiviral activities have been reported [325, 326]. PROTAC has other potential benefits, such as sub-stoichiometric activity, more selectivity and retained activity against a mutant target protein. But unlike a typical small molecule inhibitor, PROTAC molecules are generally less drug-like with a large molecular mass and various issues in pharmacokinetics and pharmacodynamics. Artificial intelligence (AI) has been rapidly evolving in recent years and could become a powerful tool for drug discovery. Given the large amount of data of *in vitro*, *in vivo* and clinical inhibition of cysteine proteases, AI could significantly contribute to the antiviral drug discovery against SARS family of coronaviruses.

Supplementary Material

Refer to Web version on PubMed Central for supplementary material.

Acknowledgement

This work was supported by grants (R21AI159323 and R01CA266057) from the United States National Institute of Health and a grant (RP220232) from Cancer Prevention and Research Institute of Texas to Y.S.

Abbreviations

SARS-CoV	severe acute respiratory syndrome-associated coronavirus
M^{Pro}	main protease
RdRp	RNA-dependent RNA polymerase
PL^{Pro}	papain-like protease
ACE2	angiotensin-converting enzyme 2
ORF	open reading frame
nsps	non-structural proteins

ERGIC	endoplasmic reticulum-Golgi intermediate compartment
CPE	cytopathic effect
HCV	hepatitis C virus
EGFR	epidermal growth factor receptor
Boc	tert-butyloxycarbonyl
EUA	Emergency Use Authorization
PROTAC	proteolysis-targeting chimera
HTS	high-throughput screening
AI	artificial intelligence

References

1. Wilder-Smith A, Chiew CJ, and Lee VJ, Can we contain the COVID-19 outbreak with the same measures as for SARS? *The lancet infectious diseases*, 2020. 20(5): p. e102–e107. [PubMed: 32145768]
2. Gates B, Responding to Covid-19—a once-in-a-century pandemic? *New England Journal of Medicine*, 2020. 382(18): p. 1677–1679. [PubMed: 32109012]
3. Sanche S, et al. , High Contagiousness and Rapid Spread of Severe Acute Respiratory Syndrome Coronavirus 2. *Emerg Infect Dis*, 2020. 26(7).
4. Zaim S, et al. , COVID-19 and multiorgan response. *Current problems in cardiology*, 2020. 45(8): p. 100618. [PubMed: 32439197]
5. Li G, et al. , Therapeutic strategies for COVID-19: progress and lessons learned. *Nature Reviews Drug Discovery*, 2023: p. 1–27.
6. Morse JS, et al. , Learning from the past: possible urgent prevention and treatment options for severe acute respiratory infections caused by 2019-nCoV. *Chembiochem*, 2020. 21(5): p. 730–738. [PubMed: 32022370]
7. V'kovski P, et al. , Coronavirus biology and replication: implications for SARS-CoV-2. *Nature Reviews Microbiology*, 2021. 19(3): p. 155–170. [PubMed: 33116300]
8. Fan K, et al. , Biosynthesis, purification, and substrate specificity of severe acute respiratory syndrome coronavirus 3C-like proteinase. *Journal of Biological Chemistry*, 2004. 279(3): p. 1637–1642. [PubMed: 14561748]
9. Pillaiyar T, Meenakshisundaram S, and Manickam M, Recent discovery and development of inhibitors targeting coronaviruses. *Drug discovery today*, 2020. 25(4): p. 668–688. [PubMed: 32006468]
10. Woo PC, et al. , Discovery of seven novel Mammalian and avian coronaviruses in the genus deltacoronavirus supports bat coronaviruses as the gene source of alphacoronavirus and betacoronavirus and avian coronaviruses as the gene source of gammacoronavirus and deltacoronavirus. *Journal of virology*, 2012. 86(7): p. 3995–4008. [PubMed: 22278237]
11. Zumla A, Hui DS, and Perlman S, Middle East respiratory syndrome. *The Lancet*, 2015. 386(9997): p. 995–1007.
12. Cui J, Li F, and Shi Z-L, Origin and evolution of pathogenic coronaviruses. *Nature reviews microbiology*, 2019. 17(3): p. 181–192. [PubMed: 30531947]
13. Kanwar A, Selvaraju S, and Esper F. Human coronavirus-HKU1 infection among adults in Cleveland, Ohio. in *Open forum infectious diseases*. 2017. Oxford University Press.

14. Smuts H, Human coronavirus NL63 infections in infants hospitalised with acute respiratory tract infections in South Africa. *Influenza and other respiratory viruses*, 2008. 2(4): p. 135–138. [PubMed: 19453465]
15. Pene F, et al. , Coronavirus 229E-related pneumonia in immunocompromised patients. *Clinical infectious diseases*, 2003. 37(7): p. 929–932. [PubMed: 13130404]
16. Walsh EE, Shin JH, and Falsey AR, Clinical impact of human coronaviruses 229E and OC43 infection in diverse adult populations. *The Journal of infectious diseases*, 2013. 208(10): p. 1634–1642. [PubMed: 23922367]
17. Wevers BA and Van Der Hoek L, Recently discovered human coronaviruses. *Clinics in laboratory medicine*, 2009. 29(4): p. 715–724. [PubMed: 19892230]
18. Vabret A, et al. , An outbreak of coronavirus OC43 respiratory infection in Normandy, France. *Clinical infectious diseases*, 2003. 36(8): p. 985–989. [PubMed: 12684910]
19. Arbour N, et al. , Neuroinvasion by human respiratory coronaviruses. *Journal of virology*, 2000. 74(19): p. 8913–8921. [PubMed: 10982334]
20. Arbour N, et al. , Persistent infection of human oligodendrocytic and neuroglial cell lines by human coronavirus 229E. *Journal of virology*, 1999. 73(4): p. 3326–3337. [PubMed: 10074187]
21. Jacomy H, et al. , Human coronavirus OC43 infection induces chronic encephalitis leading to disabilities in BALB/C mice. *Virology*, 2006. 349(2): p. 335–346. [PubMed: 16527322]
22. Bi S, et al. , Complete genome sequences of the SARS-CoV: the BJ Group (Isolates BJ01-BJ04). *Genomics, proteomics & bioinformatics*, 2003. 1(3): p. 180–192.
23. Chan JF-W, et al. , Genomic characterization of the 2019 novel human-pathogenic coronavirus isolated from a patient with atypical pneumonia after visiting Wuhan. *Emerging microbes & infections*, 2020. 9(1): p. 221–236. [PubMed: 31987001]
24. Schoeman D and Fielding BC, Coronavirus envelope protein: current knowledge. *Virology journal*, 2019. 16(1): p. 1–22. [PubMed: 30606229]
25. Astuti I, Severe Acute Respiratory Syndrome Coronavirus 2 (SARS-CoV-2): An overview of viral structure and host response. *Diabetes & Metabolic Syndrome: Clinical Research & Reviews*, 2020. 14(4): p. 407–412.
26. Ghosh AK, et al. , Drug development and medicinal chemistry efforts toward SARS-coronavirus and Covid-19 therapeutics. *ChemMedChem*, 2020. 15(11): p. 907–932. [PubMed: 32324951]
27. Ghosh AK, et al. , Progress in anti-SARS coronavirus chemistry, biology and chemotherapy. *Annual reports in medicinal chemistry*, 2006. **41**: p. 183–196. **41**
28. Harmer D, et al. , Quantitative mRNA expression profiling of ACE 2, a novel homologue of angiotensin converting enzyme. *FEBS letters*, 2002. 532(1–2): p. 107–110. [PubMed: 12459472]
29. Masters PS, The molecular biology of coronaviruses. *Advances in virus research*, 2006. 66: p. 193–292. [PubMed: 16877062]
30. Anand K, et al. , Coronavirus main proteinase (3CLpro) structure: basis for design of anti-SARS drugs. *Science*, 2003. 300(5626): p. 1763–1767. [PubMed: 12746549]
31. Pozzi C, et al. , Antitarget, Anti-SARS-CoV-2 Leads, Drugs, and the Drug Discovery–Genetics Alliance Perspective. *Journal of Medicinal Chemistry*, 2023. 66(6): p. 3664–3702. [PubMed: 36857133]
32. Zhang L, et al. , Crystal structure of SARS-CoV-2 main protease provides a basis for design of improved α -ketoamide inhibitors. *Science*, 2020. 368(6489): p. 409–412. [PubMed: 32198291]
33. Matthews DA, et al. , Structure of human rhinovirus 3C protease reveals a trypsin-like polypeptide fold, RNA-binding site, and means for cleaving precursor polyprotein. *Cell*, 1994. 77(5): p. 761–771. [PubMed: 7515772]
34. Seipelt J, et al. , The structures of picornaviral proteinases. *Virus research*, 1999. 62(2): p. 159–168. [PubMed: 10507325]
35. Dragovich PS, et al. , Structure-based design, synthesis, and biological evaluation of irreversible human rhinovirus 3C protease inhibitors. 6. Structure– activity studies of orally bioavailable, 2-pyridone-containing peptidomimetics. *Journal of medicinal chemistry*, 2002. 45(8): p. 1607–1623. [PubMed: 11931615]

36. Dragovich PS, et al. , Structure-based design, synthesis, and biological evaluation of irreversible human rhinovirus 3C protease inhibitors. Part 7: Structure–activity studies of bicyclic 2-pyridone-containing peptidomimetics. *Bioorganic & medicinal chemistry letters*, 2002. 12(5): p. 733–738. [PubMed: 11858991]
37. Dragovich PS, et al. , Structure-based design of ketone-containing, tripeptidyl human rhinovirus 3C protease inhibitors. *Bioorganic & medicinal chemistry letters*, 2000. 10(1): p. 45–48. [PubMed: 10636240]
38. Dragovich PS, et al. , Structure-based design, synthesis, and biological evaluation of irreversible human rhinovirus 3C protease inhibitors. 4. Incorporation of P1 lactam moieties as L-glutamine replacements. *Journal of medicinal chemistry*, 1999. 42(7): p. 1213–1224. [PubMed: 10197965]
39. Dragovich PS, et al. , Structure-based design, synthesis, and biological evaluation of irreversible human rhinovirus 3C protease inhibitors. 3. Structure– activity studies of ketomethylene-containing peptidomimetics. *Journal of medicinal chemistry*, 1999. 42(7): p. 1203–1212. [PubMed: 10197964]
40. Jin Z, et al. , Structure of Mpro from SARS-CoV-2 and discovery of its inhibitors. *Nature*, 2020. 582(7811): p. 289–293. [PubMed: 32272481]
41. Dai W, et al. , Structure-based design of antiviral drug candidates targeting the SARS-CoV-2 main protease. *Science*, 2020. 368(6497): p. 1331–1335. [PubMed: 32321856]
42. Dai W, et al. , Design, synthesis, and biological evaluation of peptidomimetic aldehydes as broad-spectrum inhibitors against enterovirus and SARS-CoV-2. *Journal of medicinal chemistry*, 2021. 65(4): p. 2794–2808. [PubMed: 33872498]
43. Vuong W, et al. , Feline coronavirus drug inhibits the main protease of SARS-CoV-2 and blocks virus replication. *Nature communications*, 2020. 11(1): p. 4282.
44. Fu L, et al. , Both Boceprevir and GC376 efficaciously inhibit SARS-CoV-2 by targeting its main protease. *Nature communications*, 2020. 11(1): p. 4417.
45. Iketani S, et al. , Lead compounds for the development of SARS-CoV-2 3CL protease inhibitors. *Nature communications*, 2021. 12(1): p. 2016.
46. Hung H-C, et al. , Discovery of M protease inhibitors encoded by SARS-CoV-2. *Antimicrobial agents and chemotherapy*, 2020. 64(9): p. e00872–20. [PubMed: 32669265]
47. Ma C, et al. , Boceprevir, GC-376, and calpain inhibitors II, XII inhibit SARS-CoV-2 viral replication by targeting the viral main protease. *Cell research*, 2020. 30(8): p. 678–692. [PubMed: 32541865]
48. Hu Y, et al. , Boceprevir, calpain inhibitors II and XII, and GC-376 have broad-spectrum antiviral activity against coronaviruses. *ACS Infectious Diseases*, 2021. 7(3): p. 586–597. [PubMed: 33645977]
49. Shi Y, et al. , The preclinical inhibitor GS441524 in combination with GC376 efficaciously inhibited the proliferation of SARS-CoV-2 in the mouse respiratory tract. *Emerging microbes & infections*, 2021. 10(1): p. 481–492. [PubMed: 33691601]
50. Cáceres CJ, et al. , Efficacy of GC-376 against SARS-CoV-2 virus infection in the K18 hACE2 transgenic mouse model. *Scientific Reports*, 2021. 11(1): p. 9609. [PubMed: 33953295]
51. Vuong W, et al. , Improved SARS-CoV-2 Mpro inhibitors based on feline antiviral drug GC376: Structural enhancements, increased solubility, and micellar studies. *European Journal of Medicinal Chemistry*, 2021. 222: p. 113584. [PubMed: 34118724]
52. Dampalla CS, et al. , Postinfection treatment with a protease inhibitor increases survival of mice with a fatal SARS-CoV-2 infection. *Proceedings of the National Academy of Sciences*, 2021. 118(29): p. e2101555118.
53. Rathnayake AD, et al. , 3C-like protease inhibitors block coronavirus replication in vitro and improve survival in MERS-CoV–infected mice. *Science translational medicine*, 2020. 12(557): p. eabc5332. [PubMed: 32747425]
54. Dampalla CS, et al. , Structure-guided design of conformationally constrained cyclohexane inhibitors of severe acute respiratory syndrome coronavirus-2 3CL protease. *Journal of medicinal chemistry*, 2021. 64(14): p. 10047–10058. [PubMed: 34213885]
55. Dampalla CS, et al. , Structure-guided design of direct-acting antivirals that exploit the gem-dimethyl effect and potently inhibit 3CL proteases of severe acute respiratory syndrome

- Coronavirus-2 (SARS-CoV-2) and middle east respiratory syndrome coronavirus (MERS-CoV). *European Journal of Medicinal Chemistry*, 2023. 254: p. 115376. [PubMed: 37080108]
56. Dampalla CS, et al. , Structure-guided design of potent inhibitors of SARS-CoV-2 3CL protease: Structural, biochemical, and cell-based studies. *Journal of medicinal chemistry*, 2021. 64(24): p. 17846–17865. [PubMed: 34865476]
57. Dampalla CS, et al. , Structure-guided design of potent spirocyclic inhibitors of Severe Acute Respiratory Syndrome Coronavirus-2 3C-like protease. *Journal of Medicinal Chemistry*, 2022. 65(11): p. 7818–7832. [PubMed: 35638577]
58. Dampalla CS, et al. , Broad-Spectrum Cyclopropane-Based Inhibitors of Coronavirus 3C-like Proteases: Biochemical, Structural, and Virological Studies. *ACS Pharmacology & Translational Science*, 2022.
59. Wang H, et al. , The structure-based design of peptidomimetic inhibitors against SARS-CoV-2 3C like protease as Potent anti-viral drug candidate. *European journal of medicinal chemistry*, 2022. 238: p. 114458. [PubMed: 35635946]
60. Liu H, et al. , Development of optimized drug-like small molecule inhibitors of the SARS-CoV-2 3CL protease for treatment of COVID-19. *Nature Communications*, 2022. 13(1): p. 1891.
61. Günther S, et al. , X-ray screening identifies active site and allosteric inhibitors of SARS-CoV-2 main protease. *Science*, 2021. 372(6542): p. 642–646. [PubMed: 33811162]
62. Yang S, et al. , Synthesis, crystal structure, structure– activity relationships, and antiviral activity of a potent SARS coronavirus 3CL protease inhibitor. *Journal of medicinal chemistry*, 2006. 49(16): p. 4971–4980. [PubMed: 16884309]
63. Ma XR, et al. , MPI8 is potent against SARS-CoV-2 by inhibiting dually and selectively the SARS-CoV-2 main protease and the host cathepsin L. *ChemMedChem*, 2022. 17(1): p. e202100456. [PubMed: 34242492]
64. Yang KS, et al. , A quick route to multiple highly potent SARS-CoV-2 main protease inhibitors. *ChemMedChem*, 2021. 16(6): p. 942–948. [PubMed: 33283984]
65. Ma C, et al. , Validation and invalidation of SARS-CoV-2 main protease inhibitors using the Flip-GFP and Protease-Glo luciferase assays. *Acta Pharmaceutica Sinica B*, 2022. 12(4): p. 1636–1651. [PubMed: 34745850]
66. Al-Gharabli SI, et al. , An efficient method for the synthesis of peptide aldehyde libraries employed in the discovery of reversible SARS coronavirus main protease (SARS-CoV Mpro) inhibitors. *ChemBioChem*, 2006. 7(7): p. 1048–1055. [PubMed: 16688706]
67. Zhu L, et al. , Peptide aldehyde inhibitors challenge the substrate specificity of the SARS-coronavirus main protease. *Antiviral research*, 2011. 92(2): p. 204–212. [PubMed: 21854807]
68. Akaji K, et al. , Evaluation of peptide-aldehyde inhibitors using R188I mutant of SARS 3CL protease as a proteolysis-resistant mutant. *Bioorganic & medicinal chemistry*, 2008. 16(21): p. 9400–9408. [PubMed: 18845442]
69. Akaji K, et al. , Structure-based design, synthesis, and evaluation of peptide-mimetic SARS 3CL protease inhibitors. *Journal of medicinal chemistry*, 2011. 54(23): p. 7962–7973. [PubMed: 22014094]
70. Qiao J, et al. , SARS-CoV-2 Mpro inhibitors with antiviral activity in a transgenic mouse model. *Science*, 2021. 371(6536): p. 1374–1378. [PubMed: 33602867]
71. Xia Z, et al. , Rational design of hybrid SARS-CoV-2 main protease inhibitors guided by the superimposed cocrystal structures with the peptidomimetic inhibitors GC-376, telaprevir, and boceprevir. *ACS Pharmacology & Translational Science*, 2021. 4(4): p. 1408–1421. [PubMed: 34414360]
72. Sacco MD, et al. , Structure and inhibition of the SARS-CoV-2 main protease reveal strategy for developing dual inhibitors against Mpro and cathepsin L. *Science Advances*, 2020. 6(50): p. eabe0751. [PubMed: 33158912]
73. Ma Y, et al. , A multi-pronged evaluation of aldehyde-based tripeptidyl main protease inhibitors as SARS-CoV-2 antivirals. *European Journal of Medicinal Chemistry*, 2022. 240: p. 114570. [PubMed: 35779291]

74. Costanzi E, et al. , Structural and biochemical analysis of the dual inhibition of MG-132 against SARS-CoV-2 main protease (Mpro/3CLpro) and human cathepsin-L. *International journal of molecular sciences*, 2021. 22(21): p. 11779. [PubMed: 34769210]
75. Alugubelli YR, et al. , A systematic exploration of boceprevir-based main protease inhibitors as SARS-CoV-2 antivirals. *European Journal of Medicinal Chemistry*, 2022. 240: p. 114596. [PubMed: 35839690]
76. Stefanelli I, et al. , Broad-spectrum coronavirus 3C-like protease peptidomimetic inhibitors effectively block SARS-CoV-2 replication in cells: Design, synthesis, biological evaluation, and X-ray structure determination. *European Journal of Medicinal Chemistry*, 2023. 253: p. 115311. [PubMed: 37043904]
77. Regnier T, et al. , New developments for the design, synthesis and biological evaluation of potent SARS-CoV 3CLpro inhibitors. *Bioorganic & medicinal chemistry letters*, 2009. 19(10): p. 2722–2727. [PubMed: 19362479]
78. Konno S, et al. , Design and synthesis of new tripeptide-type SARS-CoV 3CL protease inhibitors containing an electrophilic arylketone moiety. *Bioorganic & medicinal chemistry*, 2013. 21(2): p. 412–424. [PubMed: 23245752]
79. Thanigaimalai P, et al. , Design, synthesis, and biological evaluation of novel dipeptide-type SARS-CoV 3CL protease inhibitors: Structure–activity relationship study. *European journal of medicinal chemistry*, 2013. 65: p. 436–447. [PubMed: 23747811]
80. Thanigaimalai P, et al. , Development of potent dipeptide-type SARS-CoV 3CL protease inhibitors with novel P3 scaffolds: design, synthesis, biological evaluation, and docking studies. *European journal of medicinal chemistry*, 2013. 68: p. 372–384. [PubMed: 23994330]
81. Hattori S. i., et al. , A small molecule compound with an indole moiety inhibits the main protease of SARS-CoV-2 and blocks virus replication. *Nature Communications*, 2021. 12(1): p. 668.
82. Konno S, et al. , 3CL protease inhibitors with an electrophilic arylketone moiety as anti-SARS-CoV-2 agents. *Journal of Medicinal Chemistry*, 2021. 65(4): p. 2926–2939. [PubMed: 34313428]
83. Hoffman RL, et al. , Discovery of ketone-based covalent inhibitors of coronavirus 3CL proteases for the potential therapeutic treatment of COVID-19. *Journal of medicinal chemistry*, 2020. 63(21): p. 12725–12747. [PubMed: 33054210]
84. Boras B, et al., Discovery of a Novel Inhibitor of Coronavirus 3CL Protease as a Clinical Candidate for the Potential Treatment of COVID-19 (preprint). 2020.
85. Boras B, et al. , Preclinical characterization of an intravenous coronavirus 3CL protease inhibitor for the potential treatment of COVID19. *Nature Communications*, 2021. 12(1): p. 6055.
86. Owen DR, et al. , An oral SARS-CoV-2 Mpro inhibitor clinical candidate for the treatment of COVID-19. *Science*, 2021. 374(6575): p. 1586–1593. [PubMed: 34726479]
87. Vankadara S, et al. , A Warhead Substitution Study on the Coronavirus Main Protease Inhibitor Nirmatrelvir. *ACS medicinal chemistry letters*, 2022. 13(8): p. 1345–1350. [PubMed: 35971455]
88. Bai B, et al. , Peptidomimetic α -acyloxymethylketone warheads with six-membered lactam P1 glutamine mimic: SARS-CoV-2 3CL protease inhibition, coronavirus antiviral activity, and in vitro biological stability. *Journal of Medicinal Chemistry*, 2021. 65(4): p. 2905–2925. [PubMed: 34242027]
89. Steuten K, et al. , Challenges for targeting SARS-CoV-2 proteases as a therapeutic strategy for COVID-19. *ACS infectious diseases*, 2021. 7(6): p. 1457–1468. [PubMed: 33570381]
90. Zhang L, et al. , α -Ketoamides as broad-spectrum inhibitors of coronavirus and enterovirus replication: structure-based design, synthesis, and activity assessment. *Journal of medicinal chemistry*, 2020. 63(9): p. 4562–4578. [PubMed: 32045235]
91. Cooper MS, et al. , Diastereomeric Resolution Yields Highly Potent Inhibitor of SARS-CoV-2 Main Protease. *Journal of Medicinal Chemistry*, 2022. 65(19): p. 13328–13342. [PubMed: 36179320]
92. Bafna K, et al. , Hepatitis C virus drugs that inhibit SARS-CoV-2 papain-like protease synergize with remdesivir to suppress viral replication in cell culture. *Cell reports*, 2021. 35(7): p. 109133. [PubMed: 33984267]

93. Ghahremanpour MM, et al. , Identification of 14 known drugs as inhibitors of the main protease of SARS-CoV-2. *ACS medicinal chemistry letters*, 2020. 11(12): p. 2526–2533. [PubMed: 33324471]
94. Oerlemans R, et al. , Repurposing the HCV NS3–4A protease drug boceprevir as COVID-19 therapeutics. *RSC Medicinal Chemistry*, 2021. 12(3): p. 370–379.
95. Baker JD, et al. , A drug repurposing screen identifies hepatitis C antivirals as inhibitors of the SARS-CoV2 main protease. *PLoS one*, 2021. 16(2): p. e0245962. [PubMed: 33524017]
96. Kneller DW, et al. , Malleability of the SARS-CoV-2 3CL Mpro active-site cavity facilitates binding of clinical antivirals. *Structure*, 2020. 28(12): p. 1313–1320. e3. [PubMed: 33152262]
97. Westberg M, et al. , Rational design of a new class of protease inhibitors for the potential treatment of coronavirus diseases. *bioRxiv*, 2020: p. 2020.09. 15.275891.
98. Bai Y, et al. , Structural basis for the inhibition of the SARS-CoV-2 main protease by the anti-HCV drug narpaprevir. *Signal transduction and targeted therapy*, 2021. 6(1): p. 51. [PubMed: 33542181]
99. Huang C, et al. , A new generation Mpro inhibitor with potent activity against SARS-CoV-2 Omicron variants. *Signal Transduction and Targeted Therapy*, 2023. 8(1): p. 128. [PubMed: 36928316]
100. Quan B-X, et al. , An orally available Mpro inhibitor is effective against wild-type SARS-CoV-2 and variants including Omicron. *Nature Microbiology*, 2022. 7(5): p. 716–725.
101. Jain RP, et al. , Synthesis and evaluation of keto-glutamine analogues as potent inhibitors of severe acute respiratory syndrome 3CLpro. *Journal of medicinal chemistry*, 2004. 47(25): p. 6113–6116. [PubMed: 15566280]
102. Sydnés MO, et al. , Synthesis of glutamic acid and glutamine peptides possessing a trifluoromethyl ketone group as SARS-CoV 3CL protease inhibitors. *Tetrahedron*, 2006. 62(36): p. 8601–8609. [PubMed: 32287416]
103. Shao Y-M, et al. , Design, synthesis, and evaluation of trifluoromethyl ketones as inhibitors of SARS-CoV 3CL protease. *Bioorganic & medicinal chemistry*, 2008. 16(8): p. 4652–4660. [PubMed: 18329272]
104. Chou K-C, Wei D-Q, and Zhong W-Z, Binding mechanism of coronavirus main proteinase with ligands and its implication to drug design against SARS. *Biochemical and biophysical research communications*, 2003. 308(1): p. 148–151. [PubMed: 12890493]
105. Shie J-J, et al. , Inhibition of the severe acute respiratory syndrome 3CL protease by peptidomimetic α , β -unsaturated esters. *Bioorganic & medicinal chemistry*, 2005. 13(17): p. 5240–5252. [PubMed: 15994085]
106. Vatansever EC, et al. , Bepridil is potent against SARS-CoV-2 in vitro. *Proceedings of the National Academy of Sciences*, 2021. 118(10): p. e2012201118.
107. Xie X, et al. , A nanoluciferase SARS-CoV-2 for rapid neutralization testing and screening of anti-infective drugs for COVID-19. *Nature communications*, 2020. 11(1): p. 5214.
108. Yang H, et al. , Design of wide-spectrum inhibitors targeting coronavirus main proteases. *PLoS biology*, 2005. 3(10): p. e324. [PubMed: 16128623]
109. Lee C-C, et al. , Structural basis of inhibition specificities of 3C and 3C-like proteases by zinc-coordinating and peptidomimetic compounds. *Journal of Biological Chemistry*, 2009. 284(12): p. 7646–7655. [PubMed: 19144641]
110. Mondal S, et al. , Dual Inhibitors of Main Protease (MPro) and Cathepsin L as Potent Antivirals against SARS-CoV2. *Journal of the American Chemical Society*, 2022. 144(46): p. 21035–21045. [PubMed: 36356199]
111. Ghosh AK, et al. , Design and synthesis of peptidomimetic severe acute respiratory syndrome chymotrypsin-like protease inhibitors. *Journal of medicinal chemistry*, 2005. 48(22): p. 6767–6771. [PubMed: 16250632]
112. Ghosh AK, et al. , Structure-based design, synthesis, and biological evaluation of peptidomimetic SARS-CoV 3CLpro inhibitors. *Bioorganic & medicinal chemistry letters*, 2007. 17(21): p. 5876–5880. [PubMed: 17855091]
113. Amendola G, et al. , Lead discovery of SARS-CoV-2 main protease inhibitors through covalent docking-based virtual screening. *Journal of Chemical Information and Modeling*, 2021. 61(4): p. 2062–2073. [PubMed: 33784094]

114. Previti S, et al. , Structure-based lead optimization of peptide-based vinyl methyl ketones as SARS-CoV-2 main protease inhibitors. *European Journal of Medicinal Chemistry*, 2023. 247: p. 115021. [PubMed: 36549112]
115. Khatua K, et al. . An Azapeptide Platform in Conjunction with Covalent Warheads to Uncover High-Potency Inhibitors for SARS-CoV-2 Main Protease. *bioRxiv*, 2023: p. 2023.04. 11.536467.
116. Zaidman D, et al. . An automatic pipeline for the design of irreversible derivatives identifies a potent SARS-CoV-2 Mpro inhibitor. *Cell chemical biology*, 2021. 28(12): p. 1795–1806. e5. [PubMed: 34174194]
117. Stille JK, et al. , Design, synthesis and in vitro evaluation of novel SARS-CoV-2 3CLpro covalent inhibitors. *European Journal of Medicinal Chemistry*, 2022. 229: p. 114046. [PubMed: 34995923]
118. Rut W, et al. , SARS-CoV-2 Mpro inhibitors and activity-based probes for patient-sample imaging. *Nature chemical biology*, 2021. 17(2): p. 222–228. [PubMed: 33093684]
119. Ma C, et al. , Discovery of di-and trihaloacetamides as covalent SARS-CoV-2 main protease inhibitors with high target specificity. *Journal of the American Chemical Society*, 2021. 143(49): p. 20697–20709. [PubMed: 34860011]
120. Di Sarno V, et al. , Identification of a dual acting SARS-CoV-2 proteases inhibitor through in silico design and step-by-step biological characterization. *European Journal of Medicinal Chemistry*, 2021. 226: p. 113863. [PubMed: 34571172]
121. Yang H, et al. , The crystal structures of severe acute respiratory syndrome virus main protease and its complex with an inhibitor. *Proceedings of the National Academy of Sciences*, 2003. 100(23): p. 13190–13195.
122. Bacha U, et al. , Development of broad-spectrum halomethyl ketone inhibitors against coronavirus main protease 3CLpro. *Chemical biology & drug design*, 2008. 72(1): p. 34–49. [PubMed: 18611220]
123. Yamane D, et al. , Selective covalent targeting of SARS-CoV-2 main protease by enantiopure chlorofluoroacetamide. *Chemical Science*, 2022. 13(10): p. 3027–3034. [PubMed: 35432850]
124. Milligan JC, et al. , Identifying SARS-CoV-2 antiviral compounds by screening for small molecule inhibitors of Nsp5 main protease. *Biochemical Journal*, 2021. 478(13): p. 2499–2515. [PubMed: 34198327]
125. Catlin N, et al. , Reproductive and developmental safety of nirmatrelvir (PF-07321332), an oral SARS-CoV-2 Mpro inhibitor in animal models. *Reproductive Toxicology*, 2022. 108: p. 56–61. [PubMed: 35101563]
126. Kneller DW, et al. , Covalent nirmatrelvir- and boceprevir-derived hybrid inhibitors of SARS-CoV-2 main protease. *Nature communications*, 2022. 13(1): p. 2268.
127. Bai B, et al. , Peptidomimetic nitrile warheads as SARS-CoV-2 3CL protease inhibitors. *RSC Medicinal Chemistry*, 2021. 12(10): p. 1722–1730. [PubMed: 34778773]
128. Chuck C-P, et al. , Design, synthesis and crystallographic analysis of nitrile-based broad-spectrum peptidomimetic inhibitors for coronavirus 3C-like proteases. *European journal of medicinal chemistry*, 2013. 59: p. 1–6. [PubMed: 23202846]
129. Chuck C, et al. , Profiling of substrate-specificity and rational design of broadspectrum peptidomimetic inhibitors for main proteases of coronaviruses. *Hong Kong Med J*, 2014. 20(4): p. 22–25. [PubMed: 25224114]
130. Breidenbach J, et al. , Targeting the main protease of SARS-CoV-2: from the establishment of high throughput screening to the design of tailored inhibitors. *Angewandte Chemie International Edition*, 2021. 60(18): p. 10423–10429. [PubMed: 33655614]
131. Goetz D, et al. , Substrate specificity profiling and identification of a new class of inhibitor for the major protease of the SARS coronavirus. *Biochemistry*, 2007. 46(30): p. 8744–8752. [PubMed: 17605471]
132. Gan Y-R, et al. , Synthesis and activity of an octapeptide inhibitor designed for SARS coronavirus main proteinase. *Peptides*, 2006. 27(4): p. 622–625. [PubMed: 16242214]
133. Wei P, et al. , The N-terminal octapeptide acts as a dimerization inhibitor of SARS coronavirus 3C-like proteinase. *Biochemical and biophysical research communications*, 2006. 339(3): p. 865–872. [PubMed: 16329994]

134. Wu C-Y, et al. , Small molecules targeting severe acute respiratory syndrome human coronavirus. *Proceedings of the National Academy of Sciences*, 2004. 101(27): p. 10012–10017.
135. Shao YM, et al. , Structure-based design and synthesis of highly potent SARS-CoV 3CL protease inhibitors. *ChemBioChem*, 2007. 8(14): p. 1654–1657. [PubMed: 17722121]
136. Martina E, et al. , Screening of electrophilic compounds yields an aziridinyl peptide as new active-site directed SARS-CoV main protease inhibitor. *Bioorganic & medicinal chemistry letters*, 2005. 15(24): p. 5365–5369. [PubMed: 16216498]
137. Lee T-W, et al. , Crystal structures of the main peptidase from the SARS coronavirus inhibited by a substrate-like aza-peptide epoxide. *Journal of molecular biology*, 2005. 353(5): p. 1137–1151. [PubMed: 16219322]
138. Tripathi PK, et al. , Screening and evaluation of approved drugs as inhibitors of main protease of SARS-CoV-2. *International journal of biological macromolecules*, 2020. 164: p. 2622–2631. [PubMed: 32853604]
139. Konno H, et al. , Design and synthesis of a series of serine derivatives as small molecule inhibitors of the SARS coronavirus 3CL protease. *Bioorganic & Medicinal Chemistry*, 2016. 24(6): p. 1241–1254. [PubMed: 26879854]
140. Konno H, et al. , Synthesis and evaluation of phenylisoserine derivatives for the SARS-CoV 3CL protease inhibitor. *Bioorganic & Medicinal Chemistry Letters*, 2017. 27(12): p. 2746–2751. [PubMed: 28454669]
141. Jacobs J, et al. , Discovery, synthesis, and structure-based optimization of a series of N-(tert-butyl)-2-(N-arylamido)-2-(pyridin-3-yl) acetamides (ML188) as potent noncovalent small molecule inhibitors of the severe acute respiratory syndrome coronavirus (SARS-CoV) 3CL protease. *Journal of medicinal chemistry*, 2013. 56(2): p. 534–546. [PubMed: 23231439]
142. Lockbaum GJ, et al. , Crystal structure of SARS-CoV-2 main protease in complex with the non-covalent inhibitor ML188. *Viruses*, 2021. 13(2): p. 174. [PubMed: 33503819]
143. Kitamura N, et al. , Expedited approach toward the rational design of noncovalent SARS-CoV-2 main protease inhibitors. *Journal of medicinal chemistry*, 2021. 65(4): p. 2848–2865. [PubMed: 33891389]
144. Fintelman-Rodrigues N, et al. , Atazanavir, alone or in combination with ritonavir, inhibits SARS-CoV-2 replication and proinflammatory cytokine production. *Antimicrobial agents and chemotherapy*, 2020. 64(10): p. e00825–20. [PubMed: 32759267]
145. Chaves OA, et al. , Atazanavir is a competitive inhibitor of SARS-CoV-2 Mpro, impairing variants replication in vitro and in vivo. *Pharmaceuticals*, 2022. 15(1): p. 21.
146. Gupta A, et al. , Structure-based virtual screening and biochemical validation to discover a potential inhibitor of the SARS-CoV-2 main protease. *ACS omega*, 2020. 5(51): p. 33151–33161. [PubMed: 33398250]
147. Ma C and Wang J, Dipyridamole, chloroquine, montelukast sodium, candesartan, oxytetracycline, and atazanavir are not SARS-CoV-2 main protease inhibitors. *Proceedings of the National Academy of Sciences*, 2021. 118(8): p. e2024420118.
148. Alhakamy NA, et al. , Evaluation of the antiviral activity of sitagliptin-glatiramer acetate nano-conjugates against SARS-CoV-2 virus. *Pharmaceuticals*, 2021. 14(3): p. 178. [PubMed: 33668390]
149. Su H, et al. , Discovery of baicalin and baicalein as novel, natural product inhibitors of SARS-CoV-2 3CL protease in vitro. *BioRxiv*, 2020: p. 2020.04. 13.038687.
150. Su H. x., et al. , Anti-SARS-CoV-2 activities in vitro of Shuanghuanglian preparations and bioactive ingredients. *Acta Pharmacologica Sinica*, 2020. 41(9): p. 1167–1177. [PubMed: 32737471]
151. Liu H, et al. , Scutellaria baicalensis extract and baicalein inhibit replication of SARS-CoV-2 and its 3C-like protease in vitro. *Journal of Enzyme Inhibition and Medicinal Chemistry*, 2021. 36(1): p. 497–503. [PubMed: 33491508]
152. Su H, et al. , Identification of pyrogallol as a warhead in design of covalent inhibitors for the SARS-CoV-2 3CL protease. *Nature communications*, 2021. 12(1): p. 3623.

153. Xiong Y, et al. , Flavonoids in *Ampelopsis grossedentata* as covalent inhibitors of SARS-CoV-2 3CLpro: Inhibition potentials, covalent binding sites and inhibitory mechanisms. *International Journal of Biological Macromolecules*, 2021. 187: p. 976–987. [PubMed: 34333006]
154. Hamill P, et al. , Development of a red-shifted fluorescence-based assay for SARS-coronavirus 3CL protease: identification of a novel class of anti-SARS agents from the tropical marine sponge *Axinella corrugata*. 2006.
155. Lin C-W, et al. , Anti-SARS coronavirus 3C-like protease effects of *Isatis indigotica* root and plant-derived phenolic compounds. *Antiviral research*, 2005. 68(1): p. 36–42. [PubMed: 16115693]
156. Ryu YB, et al. , Biflavonoids from *Torreya nucifera* displaying SARS-CoV 3CLpro inhibition. *Bioorganic & medicinal chemistry*, 2010. 18(22): p. 7940–7947. [PubMed: 20934345]
157. Nguyen TTH, et al. , Flavonoid-mediated inhibition of SARS coronavirus 3C-like protease expressed in *Pichia pastoris*. *Biotechnology letters*, 2012. 34: p. 831–838. [PubMed: 22350287]
158. Jo S, et al. , Inhibition of SARS-CoV 3CL protease by flavonoids. *Journal of enzyme inhibition and medicinal chemistry*, 2020. 35(1): p. 145–151. [PubMed: 31724441]
159. Jo S, et al. , Flavonoids with inhibitory activity against SARS-CoV-2 3CLpro. *Journal of Enzyme Inhibition and Medicinal Chemistry*, 2020. 35(1): p. 1539–1544. [PubMed: 32746637]
160. Chen C-N, et al. , Inhibition of SARS-CoV 3C-like protease activity by theaflavin-3, 3'-digallate (TF3). *Evidence-Based Complementary and Alternative Medicine*, 2005. 2(2): p. 209–215. [PubMed: 15937562]
161. Jang M, et al. , Tea polyphenols EGCG and theaflavin inhibit the activity of SARS-CoV-2 3CL-protease in vitro. *Evidence-based complementary and alternative medicine: eCAM*, 2020. 2020.
162. Du A, et al. , Epigallocatechin-3-gallate, an active ingredient of Traditional Chinese Medicines, inhibits the 3CLpro activity of SARS-CoV-2. *International journal of biological macromolecules*, 2021. 176: p. 1–12. [PubMed: 33548314]
163. Chiou W-C, et al. , The inhibitory effects of PGG and EGCG against the SARS-CoV-2 3C-like protease. *Biochemical and Biophysical Research Communications*, 2022. 591: p. 130–136. [PubMed: 33454058]
164. Chen L, et al. , Binding interaction of quercetin-3- β -galactoside and its synthetic derivatives with SARS-CoV 3CLpro: Structure–activity relationship studies reveal salient pharmacophore features. *Bioorganic & medicinal chemistry*, 2006. 14(24): p. 8295–8306. [PubMed: 17046271]
165. Abian O, et al. , Structural stability of SARS-CoV-2 3CLpro and identification of quercetin as an inhibitor by experimental screening. *International journal of biological macromolecules*, 2020. 164: p. 1693–1703. [PubMed: 32745548]
166. Chen L, et al. , Discovering severe acute respiratory syndrome coronavirus 3CL protease inhibitors: virtual screening, surface plasmon resonance, and fluorescence resonance energy transfer assays. *Slas Discovery*, 2006. 11(8): p. 915–921.
167. Park J-Y, et al. , Chalcones isolated from *Angelica keiskei* inhibit cysteine proteases of SARS-CoV. *Journal of enzyme inhibition and medicinal chemistry*, 2016. 31(1): p. 23–30.
168. Abdallah HM, et al. , Repurposing of some natural product isolates as SARS-COV-2 main protease inhibitors via in vitro cell free and cell-based antiviral assessments and molecular modeling approaches. *Pharmaceuticals*, 2021. 14(3): p. 213. [PubMed: 33806331]
169. Rizzuti B, et al. , Rutin is a low micromolar inhibitor of SARS-CoV-2 main protease 3CLpro: Implications for drug design of quercetin analogs. *Biomedicines*, 2021. 9(4): p. 375. [PubMed: 33918402]
170. Alhadrami HA, et al. , Scaffold hopping of α -Rubromycin enables direct access to FDA-approved cromoglicic acid as a SARS-CoV-2 MPro inhibitor. *Pharmaceuticals*, 2021. 14(6): p. 541. [PubMed: 34198933]
171. Xiong Y, et al. , Discovery of naturally occurring inhibitors against SARS-CoV-2 3CLpro from *Ginkgo biloba* leaves via large-scale screening. *Fitoterapia*, 2021. 152: p. 104909. [PubMed: 33894315]
172. Consortium CM, et al. , Open science discovery of oral non-covalent SARS-CoV-2 main protease inhibitor therapeutics. *BioRxiv*, 2020: p. 2020.10. 29.339317.

173. Zhu W, et al. , Identification of SARS-CoV-2 3CL protease inhibitors by a quantitative high-throughput screening. *ACS pharmacology & translational science*, 2020. 3(5): p. 1008–1016. [PubMed: 33062953]
174. Luttens A, et al. , Ultralarge virtual screening identifies SARS-CoV-2 main protease inhibitors with broad-spectrum activity against coronaviruses. *Journal of the American Chemical Society*, 2022. 144(7): p. 2905–2920. [PubMed: 35142215]
175. Zhang K, et al. , Discovery of quinazolin-4-one-based non-covalent inhibitors targeting the severe acute respiratory syndrome coronavirus 2 main protease (SARS-CoV-2 Mpro). *European Journal of Medicinal Chemistry*, 2023: p. 115487. [PubMed: 37257212]
176. Li X, et al. , Ethacridine inhibits SARS-CoV-2 by inactivating viral particles. *PLoS pathogens*, 2021. 17(9): p. e1009898. [PubMed: 34478458]
177. Lo HS, et al. , Simeprevir potently suppresses SARS-CoV-2 replication and synergizes with remdesivir. *ACS central science*, 2021. 7(5): p. 792–802. [PubMed: 34075346]
178. Yamamoto N, et al. , HIV protease inhibitor nelfinavir inhibits replication of SARS-associated coronavirus. *Biochemical and biophysical research communications*, 2004. 318(3): p. 719–725. [PubMed: 15144898]
179. Yamamoto N, et al. , Nelfinavir inhibits replication of severe acute respiratory syndrome coronavirus 2 in vitro. *BioRxiv*, 2020: p. 2020.04. 06.026476.
180. Jan J-T, et al. , Identification of existing pharmaceuticals and herbal medicines as inhibitors of SARS-CoV-2 infection. *Proceedings of the National Academy of Sciences*, 2021. 118(5): p. e2021579118.
181. Bakowski MA, et al. , Drug repurposing screens identify chemical entities for the development of COVID-19 interventions. *Nature communications*, 2021. 12(1): p. 3309.
182. Sayed AM, et al. , Korupensamine A, but not its atropisomer, korupensamine B, inhibits SARS-CoV-2 in vitro by targeting its main protease (Mpro). *European journal of medicinal chemistry*, 2023. 251: p. 115226. [PubMed: 36893625]
183. Kuo C-J, et al. , Individual and common inhibitors of coronavirus and picornavirus main proteases. *FEBS letters*, 2009. 583(3): p. 549–555. [PubMed: 19166843]
184. Ahn T-Y, et al. , Synthesis and evaluation of benzoquinolinone derivatives as sars-cov 3cl protease inhibitors. *Bulletin of the Korean Chemical Society*, 2010. 31(1): p. 87–91.
185. Khoury E, et al., Computationally driven discovery of SARS-CoV-2 Mpro inhibitors: from design to experimental validation (preprint). 2021.
186. Li Z, et al. , Identify potent SARS-CoV-2 main protease inhibitors via accelerated free energy perturbation-based virtual screening of existing drugs. *Proceedings of the National Academy of Sciences*, 2020. 117(44): p. 27381–27387.
187. Shimamoto Y, et al. , Fused-ring structure of decahydroisoquinolin as a novel scaffold for SARS 3CL protease inhibitors. *Bioorganic & medicinal chemistry*, 2015. 23(4): p. 876–890. [PubMed: 25614110]
188. Sun Y, et al. , Synthesis and biological evaluation of quinolinone compounds as SARS CoV 3CLpro inhibitors. *Chinese Journal of Chemistry*, 2013. 31(9): p. 1199–1206. [PubMed: 32313409]
189. Mukherjee P, et al. , Structure-based virtual screening against SARS-3CLpro to identify novel non-peptidic hits. *Bioorganic & medicinal chemistry*, 2008. 16(7): p. 4138–4149. [PubMed: 18343121]
190. Mukherjee P, et al. , Inhibitors of SARS-3CLpro: virtual screening, biological evaluation, and molecular dynamics simulation studies. *Journal of chemical information and modeling*, 2011. 51(6): p. 1376–1392. [PubMed: 21604711]
191. Yoshizawa S. i., et al. , Evaluation of an octahydroisochromene scaffold used as a novel SARS 3CL protease inhibitor. *Bioorganic & medicinal chemistry*, 2020. 28(4): p. 115273. [PubMed: 31926775]
192. Ohnishi K, et al. , Evaluation of a non-prime site substituent and warheads combined with a decahydroisoquinolin scaffold as a SARS 3CL protease inhibitor. *Bioorganic & Medicinal Chemistry*, 2019. 27(2): p. 425–435. [PubMed: 30558861]

193. Li Y, et al., High-throughput Screening and Experimental Identification of Potent Drugs Targeting SARS-CoV-2 Main Protease. 2020.
194. Rossetti GG, et al. , Non-covalent SARS-CoV-2 Mpro inhibitors developed from in silico screen hits. *Scientific reports*, 2022. 12(1): p. 1–9. [PubMed: 34992227]
195. Sun Q, et al. , Bardoxolone and bardoxolone methyl, two Nrf2 activators in clinical trials, inhibit SARS-CoV-2 replication and its 3C-like protease. *Signal transduction and targeted therapy*, 2021. 6(1): p. 212. [PubMed: 34052830]
196. Hou B, et al. , Target-based virtual screening and LC/MS-guided isolation procedure for identifying phloroglucinol-terpenoid inhibitors of SARS-CoV-2. *Journal of Natural Products*, 2022. 85(2): p. 327–336. [PubMed: 35084181]
197. Wen C-C, et al. , Specific plant terpenoids and lignoids possess potent antiviral activities against severe acute respiratory syndrome coronavirus. *Journal of medicinal chemistry*, 2007. 50(17): p. 4087–4095. [PubMed: 17663539]
198. Cinatl J, et al. , Glycyrrhizin, an active component of liquorice roots, and replication of SARS-associated coronavirus. *The Lancet*, 2003. 361(9374): p. 2045–2046.
199. van de Sand L, et al. , Glycyrrhizin effectively inhibits SARS-CoV-2 replication by inhibiting the viral main protease. *Viruses*, 2021. 13(4): p. 609. [PubMed: 33918301]
200. Ryu YB, et al. , SARS-CoV 3CLpro inhibitory effects of quinone-methide triterpenes from *Tripterygium regelii*. *Bioorganic & medicinal chemistry letters*, 2010. 20(6): p. 1873–1876. [PubMed: 20167482]
201. Shi T-H, et al. , Andrographolide and its fluorescent derivative inhibit the main proteases of 2019-nCoV and SARS-CoV through covalent linkage. *Biochemical and biophysical research communications*, 2020. 533(3): p. 467–473. [PubMed: 32977949]
202. Schulte B, et al. , Andrographolide derivatives target the KEAP1/NRF2 axis and possess potent anti-SARS-CoV-2 activity. *ChemMedChem*, 2022. 17(5): p. e202100732. [PubMed: 35099120]
203. Alhadrami HA, et al. , Olive-derived triterpenes suppress SARS COV-2 main protease: a promising scaffold for future therapeutics. *Molecules*, 2021. 26(9): p. 2654. [PubMed: 34062737]
204. Ghosh AK, et al. , Design, synthesis and antiviral efficacy of a series of potent chloropyridyl ester-derived SARS-CoV 3CLpro inhibitors. *Bioorganic & medicinal chemistry letters*, 2008. 18(20): p. 5684–5688. [PubMed: 18796354]
205. Ghosh AK, et al. , Indole chloropyridinyl ester-derived SARS-CoV-2 3CLpro inhibitors: enzyme inhibition, antiviral efficacy, structure–activity relationship, and X-ray structural studies. *Journal of Medicinal Chemistry*, 2021. 64(19): p. 14702–14714. [PubMed: 34528437]
206. Hattori S. i., et al. , GRL-0920, an indole chloropyridinyl ester, completely blocks SARS-CoV-2 infection. *MBio*, 2020. 11(4): p. e01833–20. [PubMed: 32820005]
207. Zang Y, et al. , High-throughput screening of SARS-CoV-2 main and papain-like protease inhibitors. *Protein & Cell*, 2023. 14(1): p. 17–27. [PubMed: 36726755]
208. Wu C-Y, et al. , Stable benzotriazole esters as mechanism-based inactivators of the severe acute respiratory syndrome 3CL protease. *Chemistry & biology*, 2006. 13(3): p. 261–268. [PubMed: 16638531]
209. Blanchard JE, et al. , High-throughput screening identifies inhibitors of the SARS coronavirus main proteinase. *Chemistry & biology*, 2004. 11(10): p. 1445–1453. [PubMed: 15489171]
210. Zhang J, et al. , Design, synthesis, and evaluation of inhibitors for severe acute respiratory syndrome 3C-like protease based on phthalhydrazide ketones or heteroaromatic esters. *Journal of medicinal chemistry*, 2007. 50(8): p. 1850–1864. [PubMed: 17381079]
211. Niu C, et al. , Molecular docking identifies the binding of 3-chloropyridine moieties specifically to the S1 pocket of SARS-CoV Mpro. *Bioorganic & medicinal chemistry*, 2008. 16(1): p. 293–302. [PubMed: 17931870]
212. Zhang J, et al. , Aryl methylene ketones and fluorinated methylene ketones as reversible inhibitors for severe acute respiratory syndrome (SARS) 3C-like proteinase. *Bioorganic chemistry*, 2008. 36(5): p. 229–240. [PubMed: 18295820]
213. Ghosh AK, et al. , Chloropyridinyl esters of nonsteroidal anti-inflammatory agents and related derivatives as potent SARS-CoV-2 3CL protease inhibitors. *Molecules*, 2021. 26(19): p. 5782. [PubMed: 34641337]

214. Pillaiyar T, et al. , Small-molecule thioesters as SARS-CoV-2 main protease inhibitors: enzyme inhibition, structure–activity relationships, antiviral activity, and X-ray structure determination. *Journal of Medicinal Chemistry*, 2022. 65(13): p. 9376–9395. [PubMed: 35709506]
215. Verschuere KH, et al. , A structural view of the inactivation of the SARS coronavirus main proteinase by benzotriazole esters. *Chemistry & biology*, 2008. 15(6): p. 597–606. [PubMed: 18559270]
216. Brier L, et al. , Novel dithiocarbamates selectively inhibit 3CL protease of SARS-CoV-2 and other coronaviruses. *European journal of medicinal chemistry*, 2023. 250: p. 115186. [PubMed: 36796300]
217. Ma C, et al. , Ebselen, disulfiram, carmofur, PX-12, tideglusib, and shikonin are nonspecific promiscuous SARS-CoV-2 main protease inhibitors. *ACS pharmacology & translational science*, 2020. 3(6): p. 1265–1277. [PubMed: 33330841]
218. Gurard-Levin ZA, et al. , Evaluation of SARS-CoV-2 3C-like protease inhibitors using self-assembled monolayer desorption ionization mass spectrometry. *Antiviral research*, 2020. 182: p. 104924. [PubMed: 32896566]
219. Huff S, et al. , Discovery and mechanism of SARS-CoV-2 main protease inhibitors. *Journal of medicinal chemistry*, 2021. 65(4): p. 2866–2879. [PubMed: 34570513]
220. Ampornanai K, et al. , Inhibition mechanism of SARS-CoV-2 main protease by ebselen and its derivatives. *Nature communications*, 2021. 12(1): p. 3061.
221. Zmudzinski M, et al. , Ebselen derivatives are very potent dual inhibitors of SARS-CoV-2 proteases-PLpro and Mpro in in vitro studies. *BioRxiv*, 2020: p. 2020.08. 30.273979.
222. Sancineto L, et al., Organoselenium mild electrophiles in the inhibition of Mpro and SARSCoV-2 replication. 2020.
223. Sun L-Y, et al. , Ebsulfur and Ebselen as highly potent scaffolds for the development of potential SARS-CoV-2 antivirals. *Bioorganic Chemistry*, 2021. 112: p. 104889. [PubMed: 33915460]
224. Chen W, et al. , Discovery of highly potent SARS-CoV-2 Mpro inhibitors based on benzoisothiazolone scaffold. *Bioorganic & Medicinal Chemistry Letters*, 2022. 58: p. 128526. [PubMed: 34998903]
225. Qiao Z, et al. , The Mpro structure-based modifications of ebselen derivatives for improved antiviral activity against SARS-CoV-2 virus. *Bioorganic Chemistry*, 2021. 117: p. 105455. [PubMed: 34740055]
226. Guo S, et al. , Discovery of novel inhibitors against main protease (Mpro) of SARS-CoV-2 via virtual screening and biochemical evaluation. *Bioorganic Chemistry*, 2021. 110: p. 104767. [PubMed: 33667900]
227. Thun-Hohenstein ST, et al. , Structure-Activity Studies Reveal Scope for Optimisation of Ebselen-Type Inhibition of SARS-CoV-2 Main Protease. *ChemMedChem*, 2022. 17(4): p. e202100582. [PubMed: 34850566]
228. Turlington M, et al. , Discovery of N-(benzo [1, 2, 3] triazol-1-yl)-N-(benzyl) acetamido phenyl) carboxamides as severe acute respiratory syndrome coronavirus (SARS-CoV) 3CLpro inhibitors: identification of ML300 and noncovalent nanomolar inhibitors with an induced-fit binding. *Bioorganic & medicinal chemistry letters*, 2013. 23(22): p. 6172–6177. [PubMed: 24080461]
229. Han SH, et al. , Structure-based optimization of ML300-derived, noncovalent inhibitors targeting the severe acute respiratory syndrome coronavirus 3CL protease (SARS-CoV-2 3CLpro). *Journal of Medicinal Chemistry*, 2021. 65(4): p. 2880–2904. [PubMed: 34347470]
230. Jin Z, et al. , Structural basis for the inhibition of SARS-CoV-2 main protease by antineoplastic drug carmofur. *Nature structural & molecular biology*, 2020. 27(6): p. 529–532.
231. Zhang C-H, et al. , Potent noncovalent inhibitors of the main protease of SARS-CoV-2 from molecular sculpting of the drug perampanel guided by free energy perturbation calculations. *ACS central science*, 2021. 7(3): p. 467–475. [PubMed: 33786375]
232. Deshmukh MG, et al. , Structure-guided design of a perampanel-derived pharmacophore targeting the SARS-CoV-2 main protease. *Structure*, 2021. 29(8): p. 823–833. e5. [PubMed: 34161756]
233. Zhang C-H, et al. , Optimization of triarylpyridinone inhibitors of the main protease of SARS-CoV-2 to low-nanomolar antiviral potency. *ACS Medicinal Chemistry Letters*, 2021. 12(8): p. 1325–1332. [PubMed: 34408808]

234. Tsai K-C, et al. , Discovery of a novel family of SARS-CoV protease inhibitors by virtual screening and 3D-QSAR studies. *Journal of medicinal chemistry*, 2006. 49(12): p. 3485–3495. [PubMed: 16759091]
235. Ramajayam R, et al. , Synthesis, docking studies, and evaluation of pyrimidines as inhibitors of SARS-CoV 3CL protease. *Bioorganic & medicinal chemistry letters*, 2010. 20(12): p. 3569–3572. [PubMed: 20494577]
236. Clyde A, et al. , High-throughput virtual screening and validation of a SARS-CoV-2 main protease noncovalent inhibitor. *Journal of chemical information and modeling*, 2021. 62(1): p. 116–128. [PubMed: 34793155]
237. Kneller DW, et al. , Structural, electronic, and electrostatic determinants for inhibitor binding to subsites S1 and S2 in SARS-CoV-2 main protease. *Journal of medicinal chemistry*, 2021. 64(23): p. 17366–17383. [PubMed: 34705466]
238. Ge R, et al. , Discovery of SARS-CoV-2 main protease covalent inhibitors from a DNA-encoded library selection. *Slas Discovery*, 2022. 27(2): p. 79–85. [PubMed: 35063690]
239. Yu W, et al. , Structure-Based Design of a Dual-Targeted Covalent Inhibitor Against Papain-like and Main Proteases of SARS-CoV-2. *Journal of Medicinal Chemistry*, 2022.
240. Chiou W-C, et al. , Repurposing existing drugs: identification of SARS-CoV-2 3C-like protease inhibitors. *Journal of enzyme inhibition and medicinal chemistry*, 2021. 36(1): p. 147–153. [PubMed: 33430659]
241. Kaeppeler U, et al. , A new lead for nonpeptidic active-site-directed inhibitors of the severe acute respiratory syndrome coronavirus main protease discovered by a combination of screening and docking methods. *Journal of medicinal chemistry*, 2005. 48(22): p. 6832–6842. [PubMed: 16250642]
242. Xiong M, et al. , In silico screening-based discovery of novel covalent inhibitors of the SARS-CoV-2 3CL protease. *European Journal of Medicinal Chemistry*, 2022. 231: p. 114130. [PubMed: 35114541]
243. Moon P, et al. , Discovery of potent pyrazoline-based covalent SARS-CoV-2 main protease inhibitors. *bioRxiv*, 2022: p. 2022.03.05.483025.
244. Webber SE, et al. , Design, synthesis, and evaluation of nonpeptidic inhibitors of human rhinovirus 3C protease. *Journal of medicinal chemistry*, 1996. 39(26): p. 5072–5082. [PubMed: 8978838]
245. Chen L-R, et al. , Synthesis and evaluation of isatin derivatives as effective SARS coronavirus 3CL protease inhibitors. *Bioorganic & Medicinal Chemistry Letters*, 2005. 15(12): p. 3058–3062. [PubMed: 15896959]
246. Zhou L, et al. , Isatin compounds as noncovalent SARS coronavirus 3C-like protease inhibitors. *Journal of Medicinal Chemistry*, 2006. 49(12): p. 3440–3443. [PubMed: 16759084]
247. Liu W, et al. , Synthesis, modification and docking studies of 5-sulfonyl isatin derivatives as SARS-CoV 3C-like protease inhibitors. *Bioorganic & medicinal chemistry*, 2014. 22(1): p. 292–302. [PubMed: 24316352]
248. Liu P, et al. , Potent inhibitors of SARS-CoV-2 3C-like protease derived from N-substituted isatin compounds. *European journal of medicinal chemistry*, 2020. 206: p. 112702. [PubMed: 32798789]
249. Hsu JT-A, et al. , Evaluation of metal-conjugated compounds as inhibitors of 3CL protease of SARS-CoV. *FEBS letters*, 2004. 574(1–3): p. 116–120. [PubMed: 15358550]
250. Lee C-C, et al. , Structural basis of mercury-and zinc-conjugated complexes as SARS-CoV 3C-like protease inhibitors. *FEBS letters*, 2007. 581(28): p. 5454–5458. [PubMed: 17981158]
251. Coelho C, et al. , Biochemical screening for SARS-CoV-2 main protease inhibitors. *PloS one*, 2020. 15(10): p. e0240079. [PubMed: 33022015]
252. Karges J, et al. , ReI Tricarbonyl Complexes as Coordinate Covalent Inhibitors for the SARS-CoV-2 Main Cysteine Protease. *Angewandte Chemie International Edition*, 2021. 60(19): p. 10716–10723. [PubMed: 33606889]
253. He Z, et al. , Molecules inhibit the enzyme activity of 3-chymotrypsin-like cysteine protease of SARS-CoV-2 virus: the experimental and theory studies. *bioRxiv*, 2020: p. 2020.05.28.120642.

254. DeLaney C, et al. , Zinc thiotropolone combinations as inhibitors of the SARS-CoV-2 main protease. *Dalton Transactions*, 2021. 50(35): p. 12226–12233. [PubMed: 34396374]
255. Wang R, et al. , Orally administered bismuth drug together with N-acetyl cysteine as a broad-spectrum anti-coronavirus cocktail therapy. *Chemical science*, 2022. 13(8): p. 2238–2248. [PubMed: 35310492]
256. Unoh Y, et al. , Discovery of S-217622, a noncovalent oral SARS-CoV-2 3CL protease inhibitor clinical candidate for treating COVID-19. *Journal of medicinal chemistry*, 2022. 65(9): p. 6499–6512. [PubMed: 35352927]
257. Mukae H, et al. , A randomized phase 2/3 study of ensitrelvir, a novel oral SARS-CoV-2 3C-like protease inhibitor, in Japanese patients with mild-to-moderate COVID-19 or asymptomatic SARS-CoV-2 infection: results of the phase 2a part. *Antimicrobial Agents and Chemotherapy*, 2022. 66(10): p. e00697–22. [PubMed: 36098519]
258. Gao S, et al. , Discovery and crystallographic studies of trisubstituted piperazine derivatives as non-covalent SARS-CoV-2 main protease inhibitors with high target specificity and low toxicity. *Journal of Medicinal Chemistry*, 2022. 65(19): p. 13343–13364. [PubMed: 36107752]
259. Gao S, et al. , Discovery and Crystallographic Studies of Nonpeptidic Piperazine Derivatives as Covalent SARS-CoV-2 Main Protease Inhibitors. *Journal of Medicinal Chemistry*, 2022.
260. Cui J and Jia J, Discovery of juglone and its derivatives as potent SARS-CoV-2 main proteinase inhibitors. *European Journal of Medicinal Chemistry*, 2021. 225: p. 113789. [PubMed: 34438124]
261. Chamakuri S, et al. , DNA-encoded chemistry technology yields expedient access to SARS-CoV-2 Mpro inhibitors. *Proceedings of the National Academy of Sciences*, 2021. 118(36): p. e2111172118.
262. Vandyck K, et al. , ALG-097111, a potent and selective SARS-CoV-2 3-chymotrypsin-like cysteine protease inhibitor exhibits in vivo efficacy in a Syrian Hamster model. *Biochemical and Biophysical Research Communications*, 2021. 555: p. 134–139. [PubMed: 33813272]
263. Yang J, et al. , Structure-based discovery of novel nonpeptide inhibitors targeting SARS-CoV-2 Mpro. *Journal of Chemical Information and Modeling*, 2021. 61(8): p. 3917–3926. [PubMed: 34279924]
264. Drayman N, et al. , Masitinib is a broad coronavirus 3CL inhibitor that blocks replication of SARS-CoV-2. *Science*, 2021. 373(6557): p. 931–936. [PubMed: 34285133]
265. Liu X, et al. , Potential therapeutic effects of dipyridamole in the severely ill patients with COVID-19. *Acta Pharmaceutica Sinica B*, 2020. 10(7): p. 1205–1215. [PubMed: 32318327]
266. O'Donnell HR, et al. , Colloidal aggregators in biochemical SARS-CoV-2 repurposing screens. *Journal of medicinal chemistry*, 2021. 64(23): p. 17530–17539. [PubMed: 34812616]
267. Du R, et al. , Discovery of chebulagic acid and punicalagin as novel allosteric inhibitors of SARS-CoV-2 3CLpro. *Antiviral research*, 2021. 190: p. 105075. [PubMed: 33872675]
268. Liu Z, et al. , Virtual screening of novel noncovalent inhibitors for SARS-CoV 3C-like proteinase. *Journal of chemical information and modeling*, 2005. 45(1): p. 10–17.
269. Yu P-C, et al. , Drug Repurposing for the Identification of Compounds with Anti-SARS-CoV-2 Capability via Multiple Targets. *Pharmaceutics*, 2022. 14(1): p. 176. [PubMed: 35057070]
270. Liu Y-C, et al. , Screening of drugs by FRET analysis identifies inhibitors of SARS-CoV 3CL protease. *Biochemical and biophysical research communications*, 2005. 333(1): p. 194–199. [PubMed: 15950190]
271. Mody V, et al. , Identification of 3-chymotrypsin like protease (3CLPro) inhibitors as potential anti-SARS-CoV-2 agents. *Communications biology*, 2021. 4(1): p. 93. [PubMed: 33473151]
272. Li J, et al. , Crystal structure of SARS-CoV-2 main protease in complex with the natural product inhibitor shikonin illuminates a unique binding mode. *Science bulletin*, 2021. 66(7): p. 661. [PubMed: 33163253]
273. Lee H, et al. , Identification of novel drug scaffolds for inhibition of SARS-CoV 3-Chymotrypsin-like protease using virtual and high-throughput screenings. *Bioorganic & medicinal chemistry*, 2014. 22(1): p. 167–177. [PubMed: 24332657]

274. Nguyen TTH, et al. , Virtual screening identification of novel severe acute respiratory syndrome 3C-like protease inhibitors and in vitro confirmation. *Bioorganic & medicinal chemistry letters*, 2011. 21(10): p. 3088–3091. [PubMed: 21470860]
275. Yang Q, et al. , Design and synthesis of cinanserin analogs as severe acute respiratory syndrome coronavirus 3CL protease inhibitors. *Chemical and Pharmaceutical Bulletin*, 2008. 56(10): p. 1400–1405. [PubMed: 18827378]
276. Bacha U, et al. , Identification of novel inhibitors of the SARS coronavirus main protease 3CLpro. *Biochemistry*, 2004. 43(17): p. 4906–4912. [PubMed: 15109248]
277. Wu R-J, et al. , Chemical synthesis, crystal structure, versatile evaluation of their biological activities and molecular simulations of novel pyrithiobac derivatives. *European Journal of Medicinal Chemistry*, 2019. 167: p. 472–484. [PubMed: 30784880]
278. Lu I-L, et al. , Structure-based drug design and structural biology study of novel nonpeptide inhibitors of severe acute respiratory syndrome coronavirus main protease. *Journal of medicinal chemistry*, 2006. 49(17): p. 5154–5161. [PubMed: 16913704]
279. Schmidt MF, et al. , Sensitized detection of inhibitory fragments and iterative development of non-peptidic protease inhibitors by dynamic ligation screening. *Angewandte Chemie International Edition*, 2008. 47(17): p. 3275–3278. [PubMed: 18348134]
280. Santos LH, et al. , Structure-based identification of naphthoquinones and derivatives as novel inhibitors of main protease Mpro and papain-like protease PLpro of SARS-CoV-2. *Journal of Chemical Information and Modeling*, 2022. 62(24): p. 6553–6573. [PubMed: 35960688]
281. Shie J-J, et al. , Discovery of potent anilide inhibitors against the severe acute respiratory syndrome 3CL protease. *Journal of medicinal chemistry*, 2005. 48(13): p. 4469–4473. [PubMed: 15974598]
282. Park J-Y, et al. , Tanshinones as selective and slow-binding inhibitors for SARS-CoV cysteine proteases. *Bioorganic & medicinal chemistry*, 2012. 20(19): p. 5928–5935. [PubMed: 22884354]
283. Park J-Y, et al. , Dieckol, a SARS-CoV 3CLpro inhibitor, isolated from the edible brown algae *Ecklonia cava*. *Bioorganic & medicinal chemistry*, 2013. 21(13): p. 3730. [PubMed: 23647823]
284. Zhang J-W, et al. , Discovery of 9, 10-dihydrophenanthrene derivatives as SARS-CoV-2 3CLpro inhibitors for treating COVID-19. *European Journal of Medicinal Chemistry*, 2022. 228: p. 114030. [PubMed: 34883292]
285. Zhang Y, et al. , Structure-based discovery and structural basis of a novel broad-spectrum natural product against the main protease of coronavirus. *Journal of Virology*, 2022. 96(1): p. e01253–21. [PubMed: 34586857]
286. Alhadrami HA, et al. , Neoechinulin A as a promising SARS-CoV-2 Mpro inhibitor: In vitro and in silico study showing the ability of simulations in discerning active from inactive enzyme inhibitors. *Marine Drugs*, 2022. 20(3): p. 163. [PubMed: 35323462]
287. Thissera B, et al. , Bioguided isolation of cycloopenin analogues as potential SARS-CoV-2 Mpro inhibitors from *Penicillium citrinum* TDPEF34. *Biomolecules*, 2021. 11(9): p. 1366. [PubMed: 34572579]
288. Alhadrami HA, et al. , Cnicin as an anti-SARS-CoV-2: an integrated in silico and in vitro approach for the rapid identification of potential COVID-19 therapeutics. *Antibiotics*, 2021. 10(5): p. 542. [PubMed: 34066998]
289. Loschwitz J, et al. , Novel inhibitors of the main protease enzyme of SARS-CoV-2 identified via molecular dynamics simulation-guided in vitro assay. *Bioorganic Chemistry*, 2021. 111: p. 104862. [PubMed: 33862474]
290. Wang R, et al. , Identification of Vitamin K3 and its analogues as covalent inhibitors of SARS-CoV-2 3CLpro. *International Journal of Biological Macromolecules*, 2021. 183: p. 182–192. [PubMed: 33901557]
291. Ramajayam R, et al. , Synthesis and evaluation of pyrazolone compounds as SARS-coronavirus 3C-like protease inhibitors. *Bioorganic & medicinal chemistry*, 2010. 18(22): p. 7849–7854. [PubMed: 20947359]
292. Kumar V, et al. , Identification, synthesis and evaluation of SARS-CoV and MERS-CoV 3C-like protease inhibitors. *Bioorganic & medicinal chemistry*, 2016. 24(13): p. 3035–3042. [PubMed: 27240464]

293. Wang L, et al. , Discovery of unsymmetrical aromatic disulfides as novel inhibitors of SARS-CoV main protease: chemical synthesis, biological evaluation, molecular docking and 3D-QSAR study. *European Journal of Medicinal Chemistry*, 2017. 137: p. 450–461. [PubMed: 28624700]
294. Mohamed SF, et al. , SARS-CoV 3C-like protease inhibitors of some newly synthesized substituted pyrazoles and substituted pyrimidines based on 1-(3-aminophenyl)-3-(1Hindol-3-yl) prop-2-en-1-one. *International Journal of Pharmacology*, 2015. 11(7): p. 749–756.
295. Dooley AJ, et al. , From genome to drug lead: identification of a small-molecule inhibitor of the SARS virus. *Bioorganic & medicinal chemistry letters*, 2006. 16(4): p. 830–833. [PubMed: 16325400]
296. Severson WE, et al. , Development and validation of a high-throughput screen for inhibitors of SARS CoV and its application in screening of a 100,000-compound library. *Journal of biomolecular screening*, 2007. 12(1): p. 33–40. [PubMed: 17200104]
297. Kao RY, et al. , Identification of novel small-molecule inhibitors of severe acute respiratory syndrome-associated coronavirus by chemical genetics. *Chemistry & biology*, 2004. 11(9): p. 1293–1299. [PubMed: 15380189]
298. Kao RY, et al. , Characterization of SARS-CoV main protease and identification of biologically active small molecule inhibitors using a continuous fluorescence-based assay. *FEBS letters*, 2004. 576(3): p. 325–330. [PubMed: 15498556]
299. Franco LS, Maia RC, and Barreiro EJ, Identification of LASSBio-1945 as an inhibitor of SARS-CoV-2 main protease (M PRO) through in silico screening supported by molecular docking and a fragment-based pharmacophore model. *RSC medicinal chemistry*, 2021. 12(1): p. 110–119. [PubMed: 34046603]
300. Malla TR, et al. , Penicillin derivatives inhibit the SARS-CoV-2 main protease by reaction with its nucleophilic cysteine. *Journal of Medicinal Chemistry*, 2022. 65(11): p. 7682–7696. [PubMed: 35549342]
301. Malla TR, et al. , Mass spectrometry reveals potential of β -lactams as SARS-CoV-2 M pro inhibitors. *Chemical Communications*, 2021. 57(12): p. 1430–1433. [PubMed: 33462575]
302. Shcherbakov D, et al. , Design and evaluation of bispidine-based SARS-CoV-2 main protease inhibitors. *ACS medicinal chemistry letters*, 2021. 13(1): p. 140–147. [PubMed: 35043075]
303. Kühn N, et al. , Discovery of potent benzoxaborole inhibitors against SARS-CoV-2 main and dengue virus proteases. *European Journal of Medicinal Chemistry*, 2022. 240: p. 114585. [PubMed: 35863275]
304. Wang L, et al. , Discovery of novel SARS-CoV-2 3CL protease covalent inhibitors using deep learning-based screen. *European journal of medicinal chemistry*, 2022. 244: p. 114803. [PubMed: 36209629]
305. Ahmed M, et al., Identification of atovaquone and mebendazole as repurposed drugs with antiviral activity against SARS-CoV-2 (version 5). 2021.
306. Chen L, et al. , Cinanserin is an inhibitor of the 3C-like proteinase of severe acute respiratory syndrome coronavirus and strongly reduces virus replication in vitro. *Journal of virology*, 2005. 79(11): p. 7095–7103. [PubMed: 15890949]
307. Jang WD, et al. , Drugs repurposed for COVID-19 by virtual screening of 6,218 drugs and cell-based assay. *Proceedings of the National Academy of Sciences*, 2021. 118(30): p. e2024302118.
308. Choy K-T, et al. , Remdesivir, lopinavir, emetine, and homoharringtonine inhibit SARS-CoV-2 replication in vitro. *Antiviral research*, 2020. 178: p. 104786. [PubMed: 32251767]
309. Park S-J, et al. , Antiviral efficacies of FDA-approved drugs against SARS-CoV-2 infection in ferrets. *MBio*, 2020. 11(3): p. e01114–20. [PubMed: 32444382]
310. Chu C, et al. , Role of lopinavir/ritonavir in the treatment of SARS: initial virological and clinical findings. *Thorax*, 2004. 59(3): p. 252–256. [PubMed: 14985565]
311. Yang KS, et al. , Repurposing Halicin as a potent covalent inhibitor for the SARS-CoV-2 main protease. *Current Research in Chemical Biology*, 2022. 2: p. 100025. [PubMed: 35815070]
312. Komatsu H, et al. , Identification of SARS-CoV-2 main protease inhibitors from FDA-approved drugs by artificial intelligence-supported activity prediction system. *Journal of Biomolecular Structure and Dynamics*, 2021: p. 1–9.

313. Eberle RJ, et al. , The repurposed drugs suramin and quinacrine cooperatively inhibit SARS-CoV-2 3CLpro in vitro. *Viruses*, 2021. 13(5): p. 873. [PubMed: 34068686]
314. Kuzikov M, et al. , Identification of inhibitors of SARS-CoV-2 3CL-pro enzymatic activity using a small molecule in vitro repurposing screen. *ACS pharmacology & translational science*, 2021. 4(3): p. 1096–1110. [PubMed: 35287429]
315. Manandhar A, et al. , Discovery of novel small-molecule inhibitors of SARS-CoV-2 main protease as potential leads for COVID-19 treatment. *Journal of Chemical Information and Modeling*, 2021. 61(9): p. 4745–4757. [PubMed: 34403259]
316. Chen Z, et al. , Ginkgolic acid and anacardic acid are specific covalent inhibitors of SARS-CoV-2 cysteine proteases. *Cell & Bioscience*, 2021. 11: p. 1–8. [PubMed: 33407894]
317. Elseginy SA, et al. , Promising anti-SARS-CoV-2 drugs by effective dual targeting against the viral and host proteases. *Bioorganic & Medicinal Chemistry Letters*, 2021. 43: p. 128099. [PubMed: 33984473]
318. Hamdy R, et al. , Iterated virtual screening-assisted antiviral and enzyme inhibition assays reveal the discovery of novel promising anti-SARS-CoV-2 with dual activity. *International Journal of Molecular Sciences*, 2021. 22(16): p. 9057. [PubMed: 34445763]
319. Hammond J, et al. , Oral nirmatrelvir for high-risk, nonhospitalized adults with Covid-19. *New England Journal of Medicine*, 2022. 386(15): p. 1397–1408. [PubMed: 35172054]
320. Najjar-Debbiny R, et al. , Effectiveness of Paxlovid in reducing severe coronavirus disease 2019 and mortality in high-risk patients. *Clinical Infectious Diseases*, 2023. 76(3): p. e342–e349. [PubMed: 35653428]
321. Lee JT, et al. , Genetic surveillance of SARS-CoV-2 Mpro reveals high sequence and structural conservation prior to the introduction of protease inhibitor Paxlovid. *Mbio*, 2022. 13(4): p. e00869–22. [PubMed: 35862764]
322. Zhou Y, et al. , Nirmatrelvir-resistant SARS-CoV-2 variants with high fitness in an infectious cell culture system. *Science Advances*, 2022. 8(51): p. eadd7197.
323. Joyce RP, Hu VW, and Wang J, The history, mechanism, and perspectives of nirmatrelvir (PF-07321332): an orally bioavailable main protease inhibitor used in combination with ritonavir to reduce COVID-19-related hospitalizations. *Medicinal Chemistry Research*, 2022. 31(10): p. 1637–1646. [PubMed: 36060104]
324. Li X and Song Y, Proteolysis-targeting chimera (PROTAC) for targeted protein degradation and cancer therapy. *Journal of hematology & oncology*, 2020. 13(1): p. 1–14. [PubMed: 31900191]
325. de Wispelaere M, et al. , Small molecule degraders of the hepatitis C virus protease reduce susceptibility to resistance mutations. *Nature communications*, 2019. 10(1): p. 3468.
326. Desantis J, et al. , Indomethacin-based PROTACs as pan-coronavirus antiviral agents. *European Journal of Medicinal Chemistry*, 2021. 226: p. 113814. [PubMed: 34534839]

Highlights

- Main protease (M^{pro}) is essential for SARS-CoV and -CoV-2 and therefore an antiviral drug target.
- Function, structure and mechanism of catalysis of M^{pro} are reviewed.
- Small-molecule inhibitors of M^{pro} and their biological activities are summarized.
- Protein-inhibitor interactions of representative compounds are described.

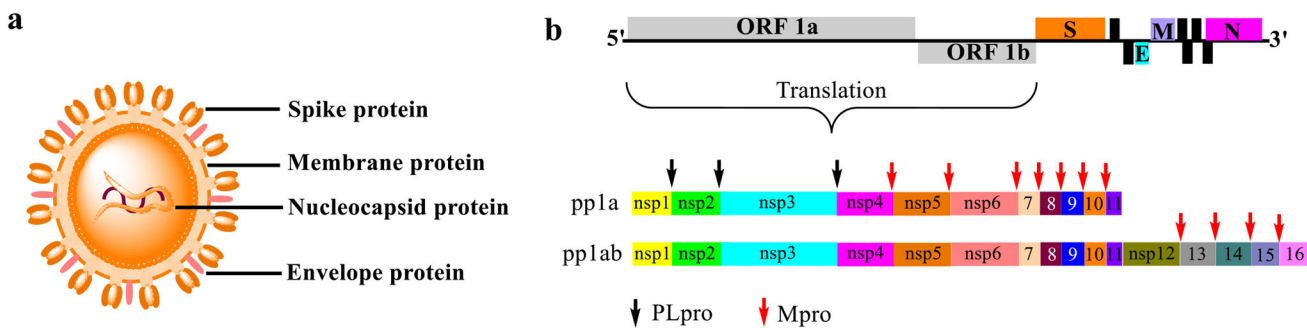


Figure 1. Schematic illustrations of (a) SARS coronavirus; and (b) The RNA genome of SARS coronavirus containing a 5'-untranslated region, 3'-untranslated region and open reading frames (ORF). ORF1a/b encode non-structure proteins (nsp) and other sequences encode the spike protein (S), envelope protein (E), membrane protein (M), nucleocapsid protein (N) and several accessory proteins (in black). The viral polyproteins (pp1a and pp1ab) translated from ORF1a/b are site-specifically cleaved by the viral M^{Pro} (nsp5, red arrows) and PL^{Pro} (nsp3, black arrows) to give viral non-structure proteins.

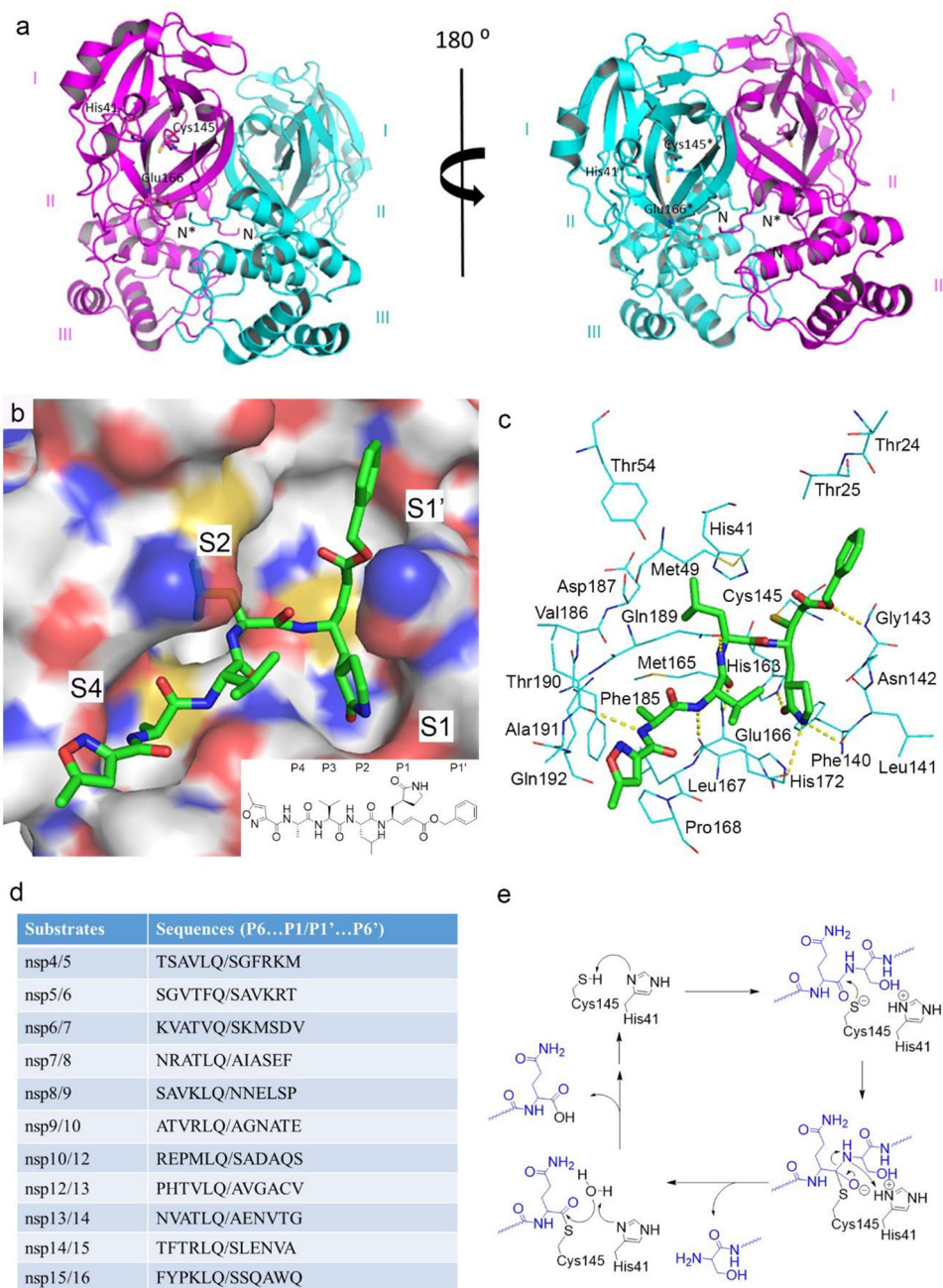


Figure 2. SARS-CoV-2 M^{Pro} structure, substrates and mechanism of catalysis. (a) The homodimeric structure of SARS-CoV-2 M^{Pro} (PDB: 6Y2G), with one monomer shown in cyan and the other in magentas. (b) The active site of M^{Pro}-N3 complex (PDB: 6LU7), with M^{Pro} shown as an electrostatic surface and N3 as a tube model with C atoms in green; (c) The M^{Pro}-N3 interactions with hydrogen bonds shown as dashed lines. Cys145 forms a covalent bond with the inhibitor; (d) Sequences of the SARS-CoV-2 M^{Pro} substrates; (e) Mechanism of catalysis for M^{Pro}.

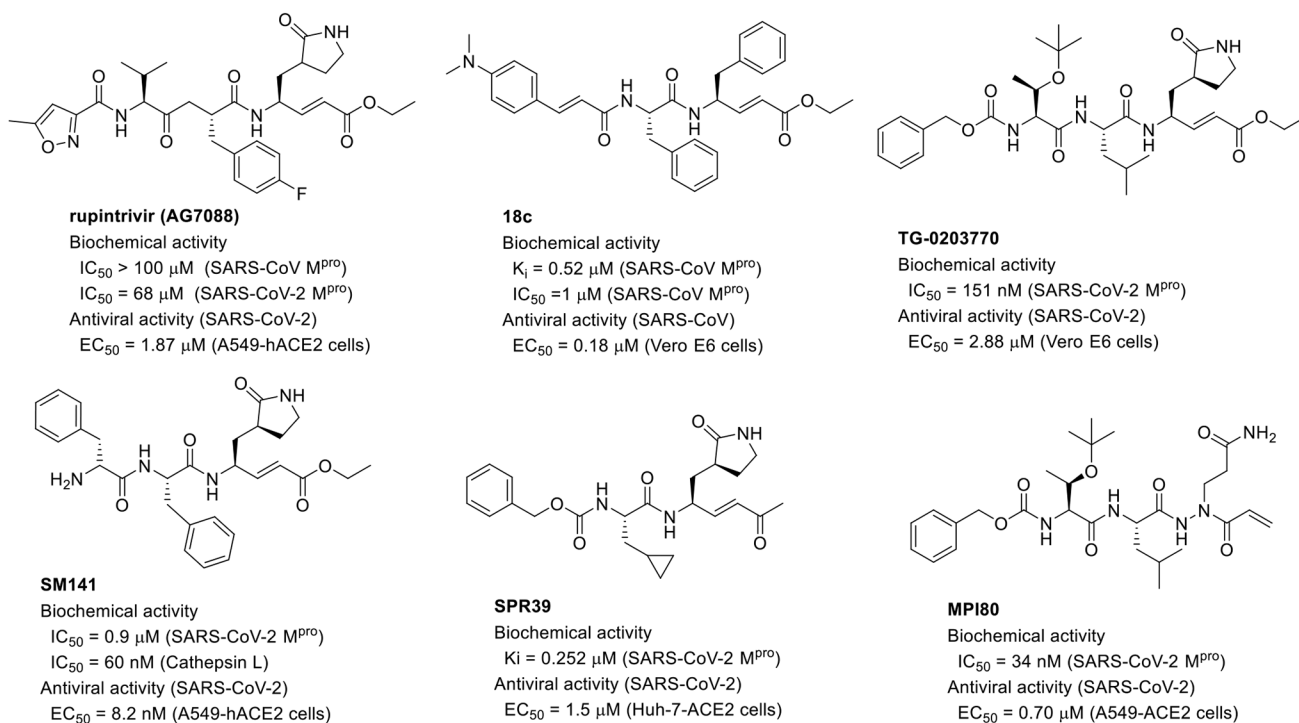


Figure 5. Structures and biological activities of α , β -unsaturated ester inhibitors of M^{pro} .

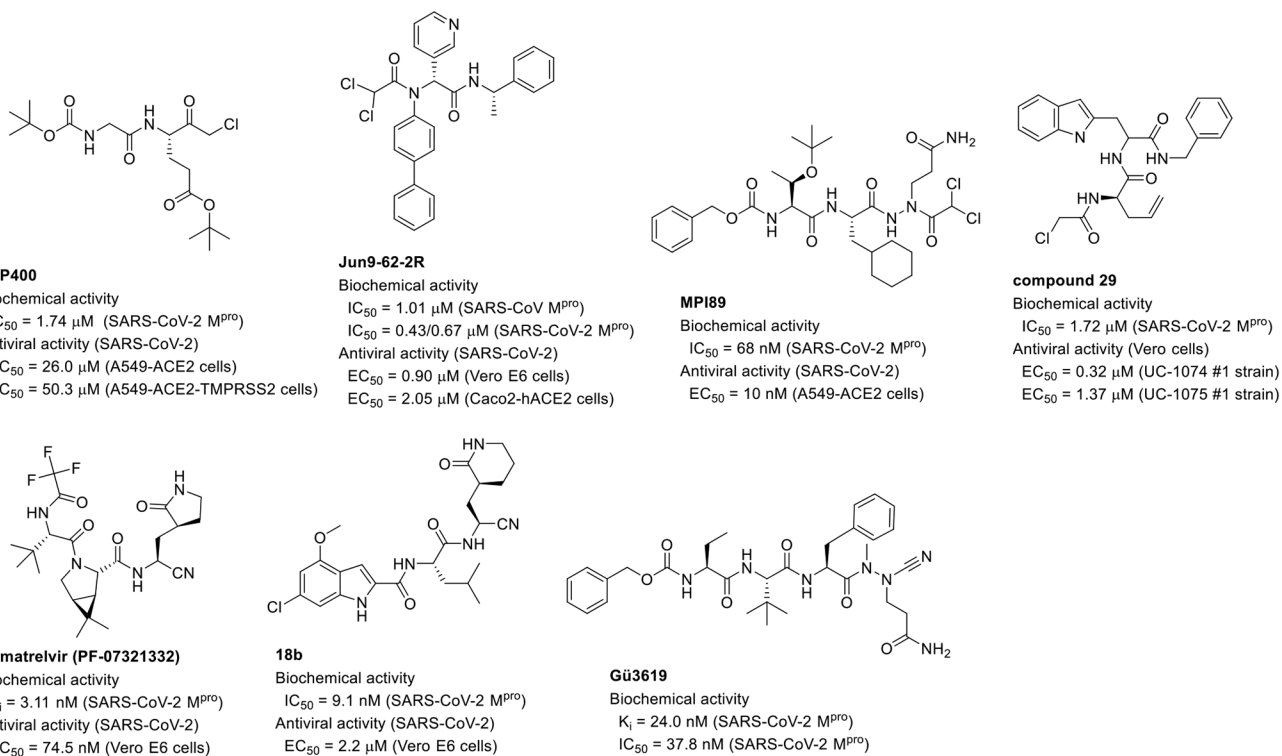
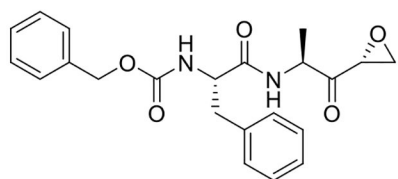


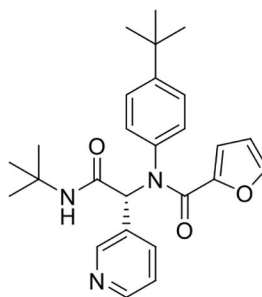
Figure 6. Structures and biological activities of haloacetyl- and nitrile-based peptidomimetic inhibitors of M^{Pro}.

**WRR183**

Biochemical activity

 $K_i = 2.2 \mu\text{M}$ (SARS-CoV M^{pro})

Antiviral activity (SARS-CoV)

 $EC_{50} = 12 \mu\text{M}$ (Vero E6 cells)**ML188**

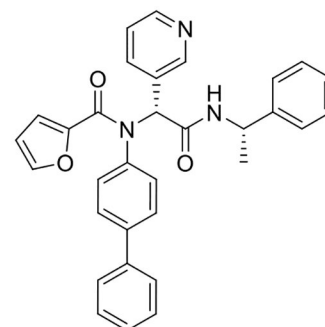
Biochemical activity

 $IC_{50} = 1.5\text{-}4.5 \mu\text{M}$ (SARS-CoV M^{pro}) $K_i = 1.6 \mu\text{M}$ (SARS-CoV M^{pro}) $IC_{50} = 2.5 \mu\text{M}$ (SARS-CoV-2 M^{pro})

Antiviral activity (SARS-CoV)

 $EC_{50} = 13 \mu\text{M}$ (Vero E6 cells)

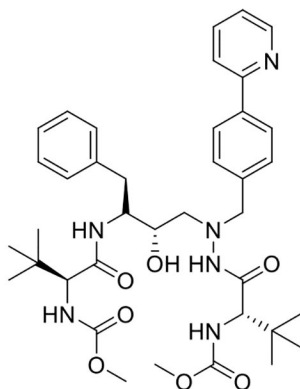
Antiviral activity (SARS-CoV-2)

 $EC_{50} > 20 \mu\text{M}$ (racemic, Vero E6 cells)**23R**

Biochemical activity

 $IC_{50} = 0.27 \mu\text{M}$ (SARS-CoV M^{pro}) $IC_{50} = 0.20 \mu\text{M}$ (SARS-CoV-2 M^{pro}) $K_i = 0.07 \mu\text{M}$ (SARS-CoV-2 M^{pro})

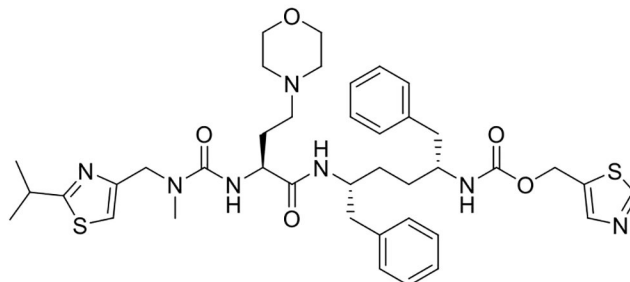
Antiviral activity (SARS-CoV-2)

 $EC_{50} = 1.27 \mu\text{M}$ (Vero E6 cells) $EC_{50} = 3.03 \mu\text{M}$ (Calu-3 cells)**atazanavir**

Biochemical activity

 $K_i = 703 \text{ nM}$ (SARS-CoV-2 M^{pro})

Antiviral activity (SARS-CoV-2)

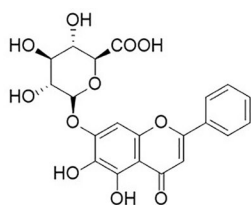
 $EC_{50} = 2.0 \mu\text{M}$ (Vero E6 cells) $EC_{50} = 0.32\text{-}0.49 \mu\text{M}$ (Calu3 cells, different variants)**cobicistat**

Biochemical activity

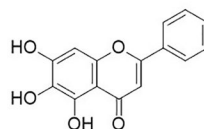
 $IC_{50} = 6.7 \mu\text{M}$ (SARS-CoV-2 M^{pro}) $K_d = 2.2 \mu\text{M}$ (SARS-CoV-2 M^{pro})

Antiviral activity (SARS-CoV-2)

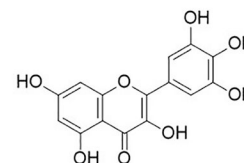
 $EC_{50} = 2.74 \mu\text{M}$ (nanoluciferase reporter assay)**Figure 7.**Structures and biological activities of the other peptidic inhibitors of M^{pro}.



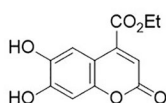
baicalin
 Biochemical activity
 $IC_{50} = 6.41 \mu\text{M}$ (SARS-CoV-2 M^{pro})
 $K_d = 11.50 \mu\text{M}$ (FRET assay)
 $K_d = 12.73 \mu\text{M}$ (MS analysis)
 Antiviral activity (SARS-CoV-2)
 $EC_{50} = 27.87 \mu\text{M}$ (Vero E6 cells)



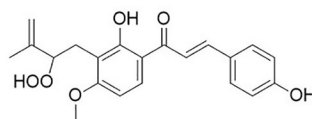
baicalein
 Biochemical activity
 $IC_{50} = 1.18 \mu\text{M}$ (SARS-CoV M^{pro})
 $IC_{50} = 0.94 \mu\text{M}$ (SARS-CoV-2 M^{pro})
 $K_d = 4.03 \mu\text{M}$ (FRET assay)
 $K_d = 1.40 \mu\text{M}$ (MS analysis)
 Antiviral activity (SARS-CoV-2)
 $EC_{50} = 2.94 \mu\text{M}$ (Vero E6 cells)



myricetin
 Biochemical activity
 $IC_{50} = 0.63 \mu\text{M}$ (SARS-CoV-2 M^{pro})
 Antiviral activity (SARS-CoV-2)
 $EC_{50} = 8.0 \mu\text{M}$ (Vero E6 cells)

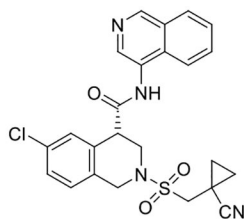


esculetin-4-carboxylic acid ethyl ester
 Biochemical activity
 $IC_{50} = 46 \mu\text{M}$ (SARS-CoV M^{pro})
 Antiviral activity (SARS-CoV)
 $EC_{50} = 112 \mu\text{M}$ (Vero E6 cells)



xanthoangelol E
 Biochemical activity (SARS-CoV M^{pro})
 $IC_{50} = 11.4 \mu\text{M}$
 $K_i = 16.1 \mu\text{M}$
 Antiviral activity (SARS-CoV Mpro)
 $EC_{50} = 7.1 \mu\text{M}$ (Vero E6 cells)

Figure 8.
 Structures and biological activities of flavonoid inhibitors of M^{pro}.

**MAT-POS-e194df51-1**

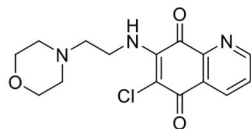
Biochemical activity

IC₅₀ = 36.8 nM (SARS-CoV-2 M^{pro})

Antiviral activity (SARS-CoV-2)

EC₅₀ = 63.8 nM (A549 cells)EC₅₀ = 149 nM (Hela-Ace2 cells)EC₅₀ = 1.15 μM (Calu-3 cells)

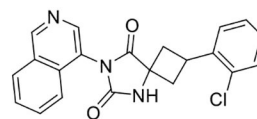
Antiviral activity (SARS-CoV-2 variants)

EC₅₀ = 0.29-1.52 μM (Hela-Ace2 cells)**DA-3003-1**

Biochemical activity

(SARS-CoV-2 M^{pro})IC₅₀ = 2.63 μM

Antiviral activity (SARS-CoV-2)

EC₅₀ = 4.47 μM (Vero E6 cells)**compound 19**

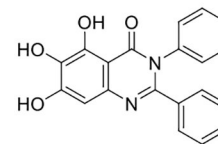
Biochemical activity

IC₅₀ = 77 nM (SARS-CoV-2 M^{pro})

Antiviral activity (SARS-CoV)

EC₅₀ = 390 nM (Vero E6 cells)

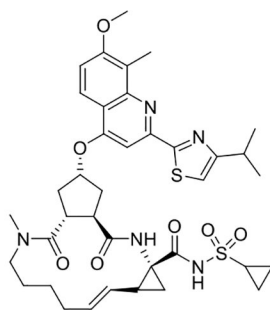
Antiviral activity (SARS-CoV-2)

EC₅₀ = 77 nM (Vero E6 cells)EC₅₀ = 110 nM (Huh7 cells)**C7**

Biochemical activity

IC₅₀ = 85 nM (SARS-CoV-2 M^{pro})

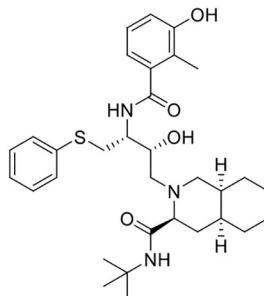
Antiviral activity (SARS-CoV-2)

EC₅₀ = 1.10 μM (Vero E6 cells)**simeprevir**

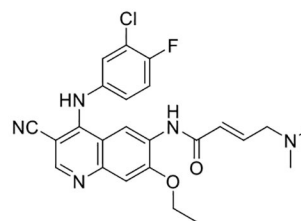
Biochemical activity

IC₅₀ = 2.46-13.74 μM (SARS-CoV-2 M^{pro})

Antiviral activity (SARS-CoV-2)

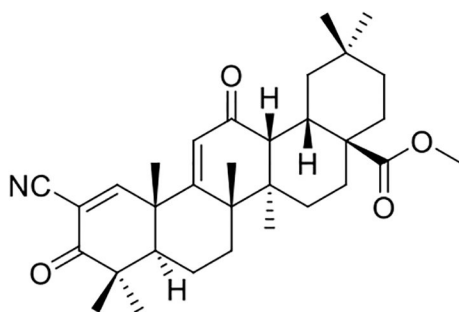
EC₅₀ = 1.40 μM (Vero E6 cells)**nelfinavir**

Antiviral activity (Vero E6 cells)

EC₅₀ = 0.048 μM (SARS-CoV)EC₅₀ = 0.77-3.3 μM (SARS-CoV-2)**pelitinib**

Antiviral activity (SARS-CoV-2)

EC₅₀ = 1.25 μM (Vero E6 cells)**Figure 9.**Structures and biological activities of quinolone and related inhibitors of M^{pro}.



bardoxolone methyl

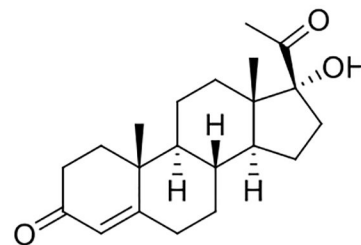
Biochemical activity

$IC_{50} = 5.81 \mu\text{M}$ (SARS-CoV-2 M^{pro})

Antiviral activity (SARS-CoV-2)

$EC_{50} = 0.29 \mu\text{M}$ (Vero cells)

$EC_{50} = 0.20 \mu\text{M}$ (Calu-3 cells)



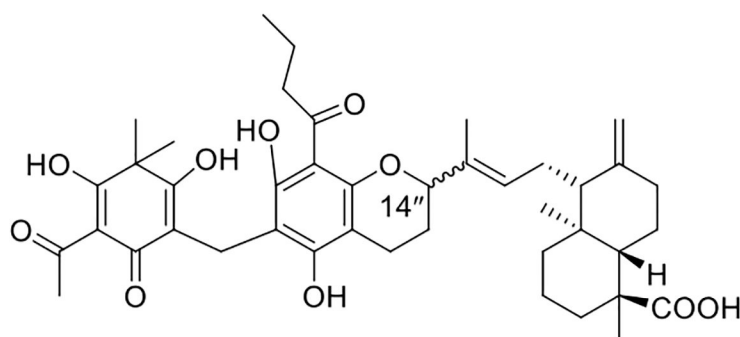
hydroxyprogesterone

Biochemical activity

$IC_{50} = 2.47 \mu\text{M}$ (SARS-CoV-2 M^{pro})

Antiviral activity (Vero E6 cells)

$EC_{50} = 2.77 \mu\text{M}$ (SARS-CoV-2)



3 (14'' S)

Biochemical activity

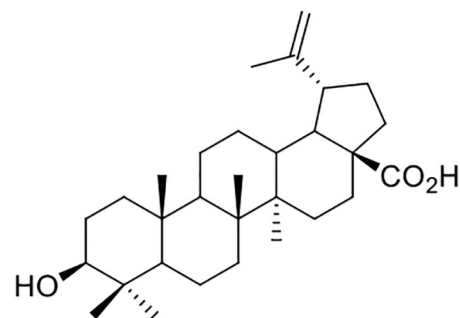
$K_d = 16.6 \mu\text{M}$ (SARS-CoV-2 M^{pro})

$IC_{50} = 7.5 \mu\text{M}$ (SARS-CoV-2 M^{pro})

Antiviral activity (SARS-CoV-2)

$EC_{50} = 4.5 \mu\text{M}$ (Vero E6 cells)

$EC_{50} = 20.2 \mu\text{M}$ (Calu-3 cells)



betulinic acid

Biochemical activity

$IC_{50} = 10 \mu\text{M}$ (SARS-CoV M^{pro})

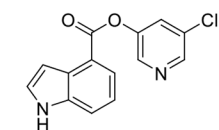
$K_i = 8.2 \mu\text{M}$ (SARS-CoV M^{pro})

Antiviral activity (SARS-CoV)

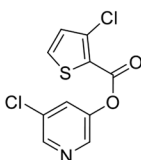
$EC_{50} > 10 \mu\text{M}$ (Vero E6 cells)

Figure 10.

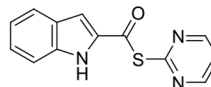
Structures and biological activities of terpenoid inhibitors of M^{pro} .

**GRL-0920**

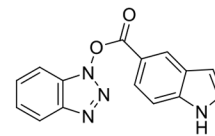
Biochemical activity
 $IC_{50} = 30 \text{ nM}$ (SARS-CoV M^{Pro})
 $IC_{50} = 0.25 \text{ }\mu\text{M}$ (SARS-CoV-2 M^{Pro})
 Antiviral activity (Vero E6 cells)
 $EC_{50} = 6.9 \text{ }\mu\text{M}$ (SARS-CoV)
 $EC_{50} = 2.8 \text{ }\mu\text{M}$ (SARS-CoV-2)

**WNN2048-F004**

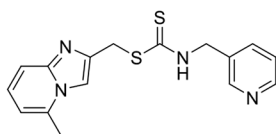
Biochemical activity
 $IC_{50} = 103.1 \text{ nM}$ (SARS-CoV-2 M^{Pro})
 Antiviral activity (SARS-CoV-2)
 $EC_{50} = 23.1 \text{ }\mu\text{M}$ (Vero cells)

**3w**

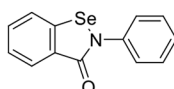
Biochemical activity
 $IC_{50} = 61.3 \text{ nM}$ (SARS-CoV M^{Pro})
 $IC_{50} = 11.4 \text{ nM}$ (SARS-CoV-2 M^{Pro})
 $K_i = 14.1 \text{ nM}$ (SARS-CoV-2 M^{Pro})
 Antiviral activity (SARS-CoV-2)
 $EC_{50} = 0.111 \text{ }\mu\text{M}$ (Calu-3 cells)

**Compound 8**

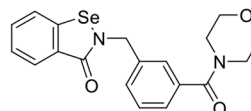
Biochemical activity
 $K_i = 7.5 \text{ nM}$ (SARS-CoV M^{Pro})

**compound 1**

Biochemical activity
 $IC_{50} = 383 \text{ nM}$ (SARS-CoV M^{Pro})
 $IC_{50} = 21 \text{ nM}$ (SARS-CoV-2 M^{Pro})
 Antiviral activity (SARS-CoV-2)
 $EC_{50} = 1.06 \text{ }\mu\text{M}$ (Vero-81 cells, with P-gp inhibition)

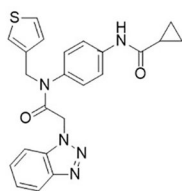
**ebselen**

Biochemical activity
 $IC_{50} = 0.67 \text{ }\mu\text{M}$ (SARS-CoV-2 M^{Pro})
 Antiviral activity (SARS-CoV-2)
 $EC_{50} = 4.67 \text{ }\mu\text{M}$ (Vero cells)

**MR6-18-4**

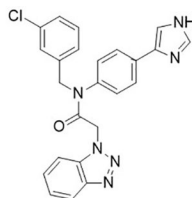
Biochemical activity
 $IC_{50} = 0.345 \text{ }\mu\text{M}$ (SARS-CoV-2 M^{Pro})
 Antiviral activity (SARS-CoV-2)
 $EC_{50} = 3.74 \text{ }\mu\text{M}$ (Vero cells)

Figure 11. Structures and biological activities of pyridinyl ester- and ebselen-based inhibitors of M^{Pro}.

**ML300**

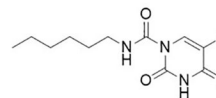
Biochemical activity

IC₅₀ = 4.11 μM (SARS-CoV M^{pro})
 IC₅₀ = 4.45 μM (SARS-CoV M^{pro})
 IC₅₀ = 4.99 μM (SARS-CoV-2 M^{pro})
 Antiviral activity (SARS-CoV-2, in Vero E6 cells)
 EC₅₀ = 19.90 μM (CPE inhibition)
 EC₅₀ = 28.15 μM (Plaque reduction)

**CCF0058981**

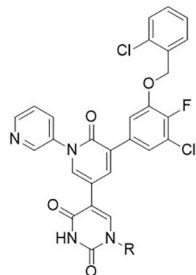
Biochemical activity

IC₅₀ = 19 nM (SARS-CoV M^{pro})
 IC₅₀ = 68 nM (SARS-CoV-2 M^{pro})
 Antiviral activity (SARS-CoV-2, in Vero E6 cells)
 EC₅₀ = 497 nM (CPE inhibition)
 EC₅₀ = 558 nM (Plaque reduction)

**carmofur**

Biochemical activity

IC₅₀ = 1.82 μM (SARS-CoV-2 M^{pro})
 Antiviral activity (SARS-CoV-2)
 EC₅₀ = 24.30 μM (Vero E6 cells)

**compound 23**, R = H

Biochemical activity

IC₅₀ = 20 nM (SARS-CoV-2 M^{pro})
 Antiviral activity (SARS-CoV-2)
 EC₅₀ = 0.84 μM (Vero E6 cells)

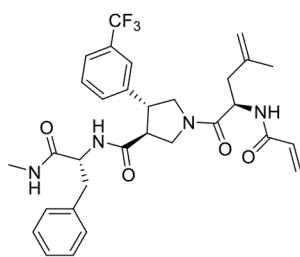
compound 19, R = Me

Biochemical activity

IC₅₀ = 44 nM (SARS-CoV-2 M^{pro})
 Antiviral activity (SARS-CoV-2)
 EC₅₀ = 80 nM (Vero E6 cells)

Figure 12.

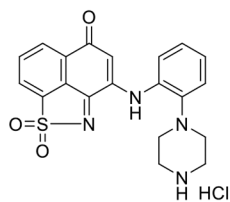
Structures and biological activities of benzotriazole- and pyrimidine-based inhibitors of M^{pro}.

**1e**

Biochemical activity

IC₅₀ = 2.0 μM (SARS-CoV-2 M^{pro})IC₅₀ = 3.5 μM (SARS-CoV M^{pro})

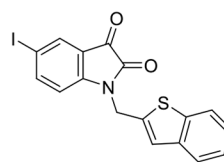
Antiviral activity (SARS-CoV-2)

EC₅₀ = 33 μM (Vero cells)**LY1**

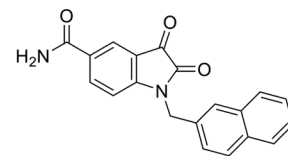
Biochemical activity

IC₅₀ = 0.12 μM (SARS-CoV-2 M^{pro})IC₅₀ = 0.99 μM (SARS-CoV-2 PL^{pro})

Antiviral activity (SARS-CoV-2)

EC₅₀ = 3.9 μM (Vero E6 cells)**4o**

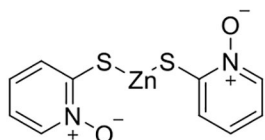
Biochemical activity

IC₅₀ = 0.95 μM (SARS-CoV M^{pro})**5f**

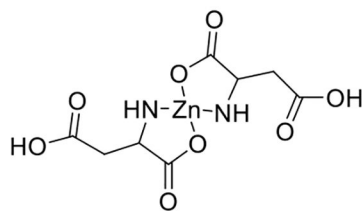
Biochemical activity

IC₅₀ = 0.37 μM (SARS-CoV M^{pro})K_i = 0.12 μM (SARS-CoV M^{pro})IC₅₀ = 45 nM (SARS-CoV-2 M^{pro})

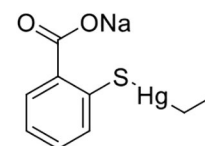
Figure 13. Structures and biological activities of acrylamide, isatin and related inhibitors of M^{pro}.

**1-hydroxypyridine-2-thione zinc**

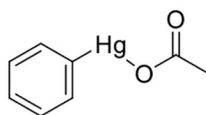
Biochemical activity

Ki = 0.17 μM (SARS-CoV-2 M^{pro})**JMF1586**

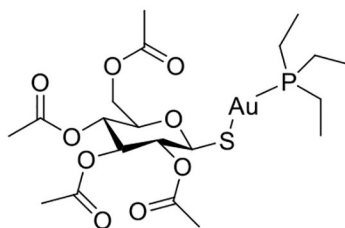
Biochemical activity

Ki = 0.05 μM (SARS-CoV M^{pro})**thimerosal**

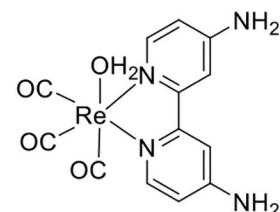
Biochemical activity

IC₅₀ = 0.6 μM (SARS-CoV-2 M^{pro})Ki = 0.6 μM (SARS-CoV-2 M^{pro})**phenylmercuric acetate**

Biochemical activity

IC₅₀ = 0.4 μM (SARS-CoV-2 M^{pro})Ki = 0.11 μM (SARS-CoV-2 M^{pro})**auranofin**

Biochemical activity

IC₅₀ = 0.51 μM (SARS-CoV-2 M^{pro})**Re^I tricarbonyl complexe**

Biochemical activity

IC₅₀ = 7.5 μM (SARS-CoV-2 M^{pro})**Figure 14.**Structures and biological activities of metal-containing inhibitors of M^{pro}.

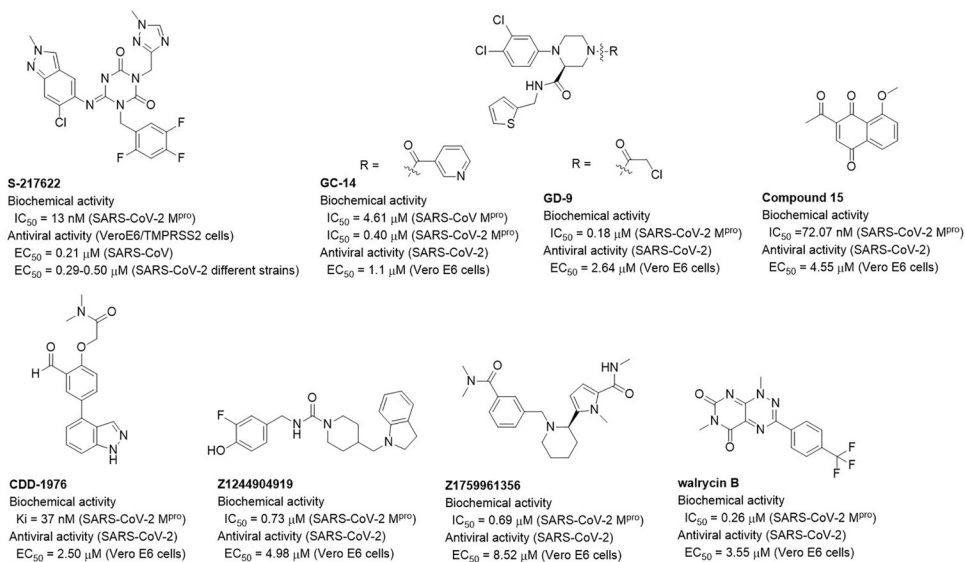
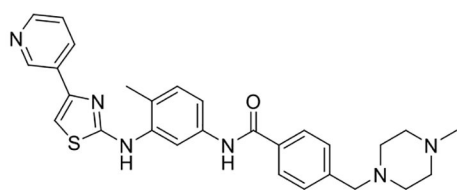


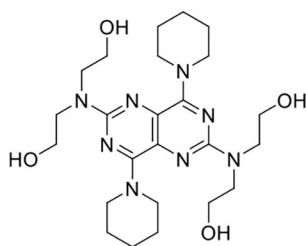
Figure 15. Structures and biological activities of triazine and other miscellaneous inhibitors of M^{pro}.

**masitinib**

Biochemical activity

 $IC_{50} = 2.5 \mu\text{M}$ (SARS-CoV-2 M^{pro})

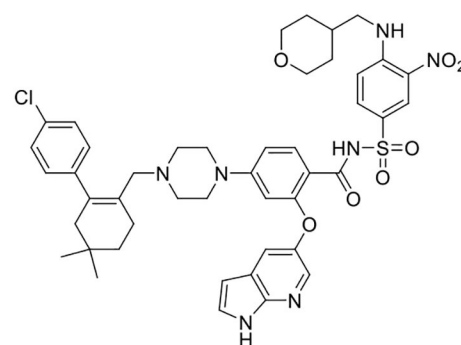
Antiviral activity (SARS-CoV-2)

 $EC_{50} = 3.2 \mu\text{M}$ (A549 cells)**dipyriddyamole**

Biochemical activity

 $IC_{50} = 0.60 \mu\text{M}$ (SARS-CoV-2 M^{pro}) $K_i = 0.04 \mu\text{M}$ (SARS-CoV-2 M^{pro})

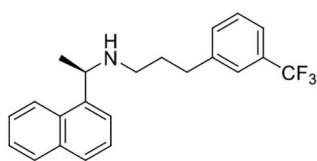
Antiviral activity (SARS-CoV-2)

 $EC_{50} = 0.1 \mu\text{M}$ (Vero E6 cells)**venetoclax**

Biochemical activity

 $IC_{50} = 3.18 \mu\text{M}$ (SARS-CoV-2 M^{pro})

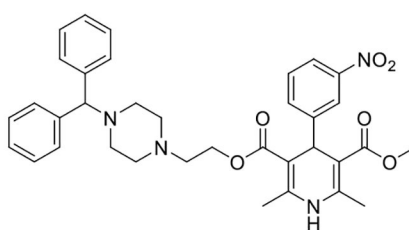
Antiviral activity (Vero E6 cells)

 $EC_{50} = 1.18 \mu\text{M}$ (SARS-CoV-2)**cinacalcet**

Biochemical activity

 $IC_{50} = 5.99 \mu\text{M}$ (SARS-CoV-2 M^{pro})

Antiviral activity (SARS-CoV-2)

 $EC_{50} = 2.93 \mu\text{M}$ (Vero E6 cells)**manidipine**

Biochemical activity

 $IC_{50} = \sim 5 \mu\text{M}$ (SARS-CoV-2 M^{pro})**Figure 16.**Structures and biological activities of clinical drugs that inhibit M^{pro}.

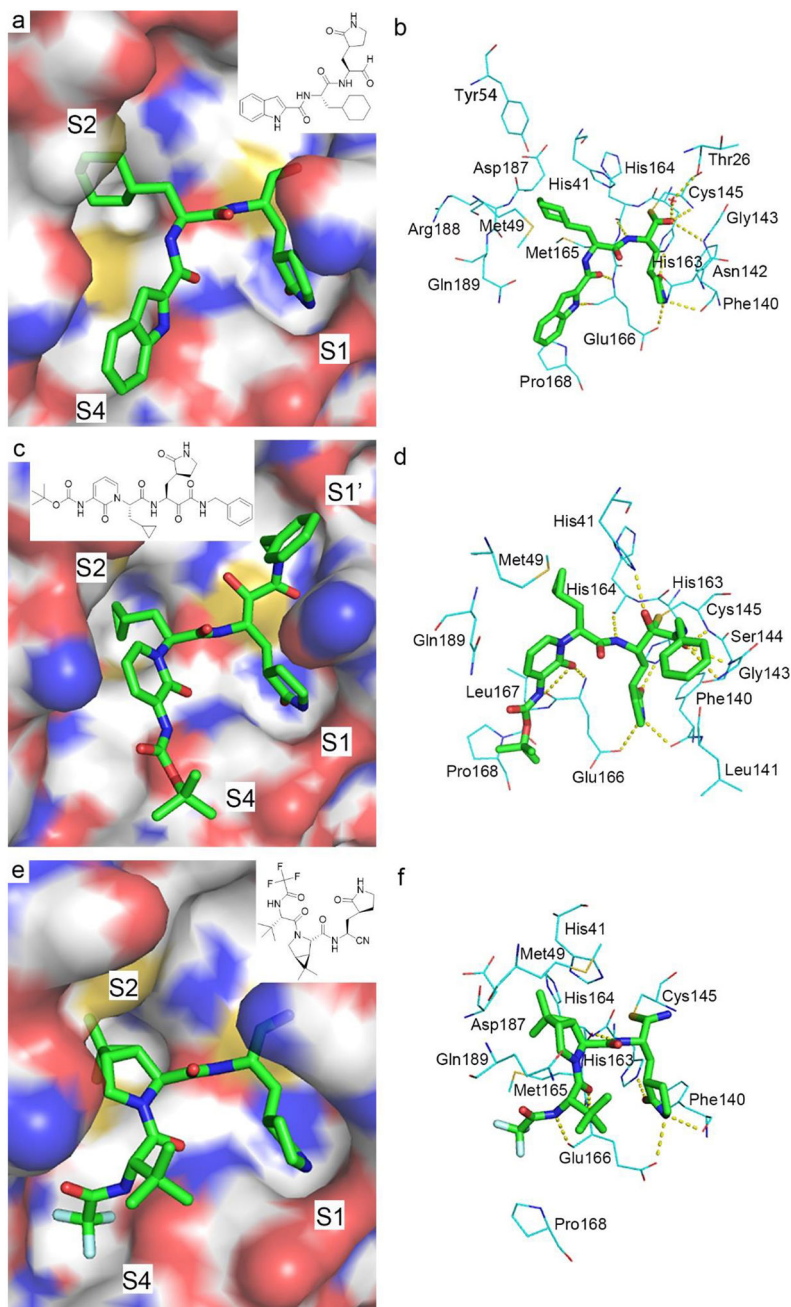


Figure 17. X-ray structures of M^{Pro} in complex with representative peptidomimetic covalent inhibitors. (a, c, e) The active site of M^{Pro} (shown as an electrostatic surface) in complex with (a) **11a** (PDB: 6LZE), (c) **13b** (PDB: 6Y2G) and (e) nirmatrelvir (PDB: 7RFW); (b, d, f) The M^{Pro} -inhibitor interactions for (b) **11a**, (d) **13b** and (f) nirmatrelvir. Hydrogen bonds are shown as yellow dashed lines.

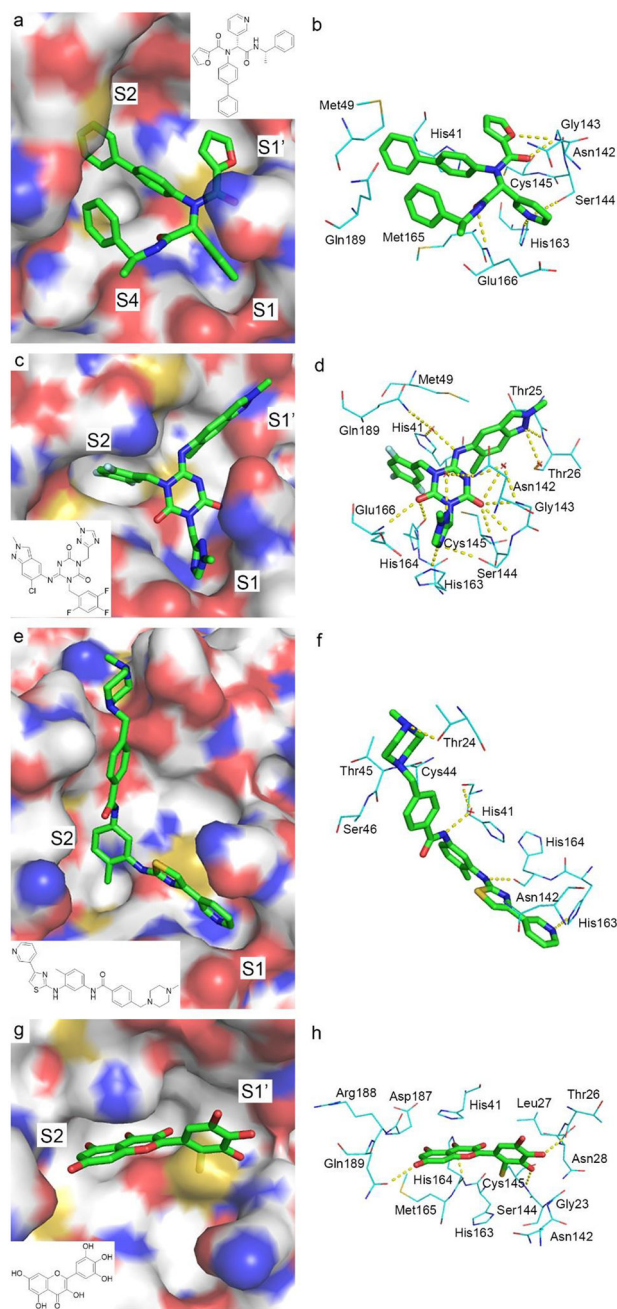


Figure 18.

X-ray structures of MPTO in complex with non-peptidic inhibitors. (a, c, e, g) The active site of MPTO (shown as an electrostatic surface) in complex with (a) 23R (PDB: 7KX5), (c) S-217622 (PDB: 7VU6), (e) masitinib (PDB: 7JU7) and (g) oxidized myricetin (PDB: 7DPP); (b, d, f, h) The MPTO-inhibitor interactions for (b) 23R, (d) S-217622, (f) masitinib and (h) oxidized myricetin. Hydrogen bonds are shown as yellow dashed lines.

Table 1.SARS-CoV and -CoV-2 M^{Pro} inhibitors in clinical trial.

Name	Clinical stage	Clinical trial identifier	Sponsor
ensitrelvir (S-217622) (Figure 15)	Approved in Japan	NCT05897541 , NCT05305547 , NCT05605093	Shionogi Inc., University of Minnesota
STI-1558	Phase I/III	NCT05523739 , NCT05716425	Zhejiang ACEA Pharmaceutical Co. Ltd.
pomotrelvir (PBI-0451)	Phase II	NCT05543707	Pardes Biosciences, Inc.
EDP-235	Phase II	NCT05616728	Enanta Pharmaceuticals, Inc.
ASC11	Phase I	NCT05718518	Ascleptis Pharmaceuticals Co., Ltd.
HS-10517	Phase II	NCT05779579	Jiangsu Hansoh Pharmaceutical Co., Ltd.
PF-07304814 (Figure 4)	Phase I	NCT04627532 , NCT04535167 , NCT05050682	Pfizer
nirmatrelvir (Figure 6) /ritonavir	Approved worldwide	NCT05668091 , NCT05576662	Harlan M Krumholz / Stanford University
montelukast	Phase II	NCT04718285	Bahcesehir University
masitinib (AB1010) (Figure 16)	Phase II	NCT05047783	AB Science